

## FINAL REPORT

### 1. ADMINISTRATIVE:

**Principal Investigator:** Thomas Giambelluca

**Institution:** UH Mānoa

**Project Title:** Understanding the response of native and non-native forests to climate variability and change to support resource management in Hawai'i

**Agreement Number:** G13AC00314

**Report Date:** 9/30/2016

**Performance Period:** 8/16/2013 - 6/30/2016

**Award Amount:** \$229,697

### 2. PUBLIC SUMMARY:

One of the biggest concerns about global climate change impacts relates to how forests and other ecosystems will be affected. Along with increasing concentrations of carbon dioxide in the atmosphere and warming temperatures, rainfall, cloud cover, storm frequency, and other aspects of climate will also change. These shifts are likely to have effects on plants, such as changing the amount of water they use or how fast they grow. In this project, we investigated the connections between environmental conditions (such as temperature, rainfall, solar radiation, humidity, wind speed, soil moisture) and plant water use and growth rates of two forest ecosystems in Hawai'i. Based on those connections, we sought to project how a specific set of possible future climate changes will affect water use and growth of these forests. The forests chosen for study represent relatively undisturbed native forest and a forest that has been invaded by the non-native tree strawberry guava. As a result of this study, we have found that more water is used at the non-native forest site, and growth characteristics of the two sites are different. Projections of changes that will be caused by future climate change show that both forests will use more water and will grow more slowly. It appears that both of these effects will be greater for the non-native site, i.e., the water use will increase more for the non-native forest and the growth will be reduced more there. Our findings are important because future increases in forest water use caused by climate change could reduce the availability of groundwater resources and streamflow. Reduced growth rates could affect forest health and stability, which could further curtail the ecosystem services they provide.

### 3. TECHNICAL SUMMARY:

This project sought to determine how projected climate change would affect ecosystem fluxes for native and non-native forests in Hawai'i. To address this goal, this project built on existing data and research infrastructure at two wet montane forest study sites in Hawai'i Volcanoes National Park, one (native) dominated by *Metrosideros polymorpha* and the other (non-native) invaded by *Psidium cattleianum*. The approach included use of flux estimates from eddy covariance measurements from each site, biometric measurements of changes in aboveground carbon storage, litterfall, and soil respiration, measurements and analysis of leaf-level gas exchange characteristics, and application of the Community Land Model (CLM) to simulate processes at the two sites. The results showed that fluxes at the two sites differ, including greater evapotranspiration, higher gross primary productivity, and much higher ecosystem respiration at the non-native forest site. Fluxes were found to be sensitive to available energy (net radiation in the case of water vapor flux and photosynthetically-active radiation, PAR, in the case of carbon uptake), atmospheric dryness (vapor pressure deficit, VPD), and leaf wetness. Gross primary production (GPP) response to PAR was much greater at the non-native site, especially during the summer. Projections of changes in ecosystem

fluxes due to future climate change showed that evapotranspiration will increase and carbon storage (growth) will decrease at both sites, with greater amplitude of those effects at the non-native site. Leaf-level measurements and analysis found no differences between the principal native and non-native tree species. This finding suggests that the observed stand-level site differences are not caused by higher fluxes of water vapor and carbon dioxide by *Psidium cattleianum*. While we cannot rule out that the differences are related to the invasion, the causes of the observed site differences are not clear. The results reported here are the first to use a combination of tower-based flux measurements, biometric estimates, leaf-level measurements, and an ecosystem model to estimate current and future water vapor and carbon exchange characteristics of Hawaiian forests. These results build on other field studies of forest carbon dynamics in Hawai'i and other tropical forest locations and contribute toward a better understanding of how climate variability and climate change affect forests and the ecosystem services they provide.

#### **4. PURPOSE AND OBJECTIVES:**

The objective of this study was to determine how projected changes in temperature, precipitation and other climate variables will influence stand growth rates and water use within two of Hawai'i's most prevalent plant communities: 'ōhi'a (*Metrosideros polymorpha*)-dominated, and strawberry guava (*Psidium cattleianum*)-dominated (the most extensive invaded forest type in Hawai'i) stands. Knowledge of the relative responses of these two dominant forest types (and their underlying keystone species) to shifts in climate is directly relevant to land conservation planning and restoration efforts and will enable more effective allocation of scarce resources in efforts to conserve forests and protect watersheds. This objective has been met by applying several strategies to detect the sensitivity of these ecosystems to climate variability and to project changes to projected climate change during this century.

#### **5. ORGANIZATION AND APPROACH:**

We employed a coupled field and modeling strategy to address the objectives of this study. The four tasks enumerated below were used to determine the sensitivity of ecosystem flux response to climate at two sites representing tropical montane wet native and non-native forests in Hawai'i: (Task 1) analyzing fine time-scale variations in water and carbon flux observations from two ecosystem flux towers in relation to relevant meteorological and hydrological variables (temperature, humidity, CO<sub>2</sub> concentration, solar radiation, PAR, wind, rainfall, soil moisture, etc.); (Task 2) conducting analysis of vegetation plot data as a means of validating eddy covariance observations of carbon exchange; (Task 3) taking leaf-level measurements to identify species-specific traits that explain differential responses to environmental forcing; and (Task 4) use the Community Land Model (CLM) to simulate carbon and water exchange at each site under current and future climate conditions. These methods were chosen to provide a comprehensive assessment of likely climate impacts on these two ecosystems.

#### **6. PROJECT RESULTS:**

Task 1: Measurement and Analysis of Meteorological and Eddy Covariance data from Native and Non-native Forest Sites in Hawai'i Volcanoes National Park (see Appendix for more details)  
The average energy closure is about 79 and 99% at Thurston and Ola'a, respectively, well within the range found for flux tower sites globally. The period of record mean LE and ET for Thurston Ola'a are given in Table 1.

Table 1. Mean annual latent energy flux and evapotranspiration.

	Thurston	Ola'a
<b>Latent energy flux (W m<sup>-2</sup>)</b>		
Unadjusted	47.04	56.76
Adjusted	57.80	61.49
<b>Evapotranspiration (mm yr<sup>-1</sup>)</b>		
Unadjusted	606	731
Adjusted	744	792
<b>Site Comparison (ratio)</b>		
Ola'a/Thurston Unadjusted	1.21	
Ola'a/Thurston Adjusted	1.06	

Mean annual carbon fluxes: ecosystem respiration ( $R_{eco}$ ), gross primary production (GPP), and net ecosystem exchange (NEE) are summarized for each site in Table 2.

Table 2. Mean annual fluxes of carbon at the Thurston and Ola'a field sites: ecosystem respiration ( $R_{eco}$ ), gross primary production (GPP), and net ecosystem exchange (NEE).

C Fluxes ( $\mu\text{mol m}^{-2} \text{s}^{-1}$ )	$R_{eco}$	GPP	NEE
Thurston	4.751	-5.864	-1.112
Ola'a	7.018	-7.895	-0.902
<b>C Fluxes (Mg ha<sup>-1</sup> yr<sup>-1</sup>)</b>			
Thurston	18.0	22.2	4.21
Ola'a	26.6	29.9	3.42
<b>Site comparison (ratio)</b>			
Ola'a/Thurston	1.48	1.35	0.81

Using multiple regression analysis and after testing of alternative predictor variable combinations, the best statistical models of LE<sub>adj</sub> are:

$$\text{Thurston: LE}_{adj} = -42.70 + 0.207 * \text{RNET} + 242.58 * \text{VPD} + 67.431 * \text{FW} \quad (1)$$

Multiple R-squared: 0.867

Residual standard error:: 4.322

$$\text{Ola'a: LE}_{adj} = -24.73 + 0.256 * \text{RNET} + 138.92 * \text{VPD} + 42.957 * \text{FW} \quad (2)$$

Multiple R-squared: 0.859

Residual standard error:: 5.152

#### *Carbon Flux Sensitivity to Variations in Environmental Conditions*

Using multiple regression analysis and after testing of alternative predictor variable combinations, the best statistical models of NEE are:

$$\text{Thurston: NEE} = 1.770 - 0.00855 * \text{PAR} + 2.2440 * \text{VPD} \quad (3)$$

Multiple R-squared: 0.705

Residual standard error: 0.451

$$\text{Ola'a: } \text{NEE} = 2.178 - 0.01553 * \text{PAR} + 10.0357 * \text{VPD} \quad (4)$$

Multiple R-squared: 0.716

Residual standard error:: 0.641

Projected changes in ET and NEE based on equations (3) - (5) are given in Tables 3 and 4.

Table 3. Projected change in evapotranspiration ( $\text{LE}_{\text{adj}}$ ; %) as a result of estimated changes in  $R_{\text{net}}$  and VPD based on multiple regression models at each site.

	$\text{LE}_{\text{adj}}$ Change from Present			
	Thurston		Ola'a	
	Wet Season	Dry Season	Wet Season	Dry Season
Scenario 1	+10.1%	+12.5%	+19.0%	+18.4%
Scenario 2	+11.7%	+14.1%	+20.1%	+14.5%

Table 4. Projected change in net ecosystem carbon exchange (NEE; %) as a result of estimated changes in PAR and VPD based on multiple regression models at each site.

	NEE Change from Present			
	Thurston		Ola'a	
	Wet Season	Dry Season	Wet Season	Dry Season
Scenario 1	-8.9%	-0.6%	-24.3%	-14.2%
Scenario 2	-3.3%	+5.0%	-17.1%	-7.5%

#### Task 2: Validation of Flux Tower Observations with Biometric Measurements

(see Appendix for more details)

Aboveground fine litterfall was 60.4% higher at the invaded than the native site (Table 5). At the invaded site, the non-native tree *P. cattleianum* accounted for 17.6% of total litterfall (Table 5). Stand level GPP estimated from litterfall showed values of  $1,121.9 \text{ g C m}^{-2} \text{ yr}^{-1}$  for the native site, and  $1,800 \text{ g C m}^{-2} \text{ yr}^{-1}$  for the invaded site, and once again the nonnative tree accounted for 17.6% of stand productivity at the invaded site (Table 5). Discounting production associated with the nonnative tree, stand level litterfall and GPP associated with native species was 32.3% higher at the invaded site (Table 5).

Table 5. Aboveground fine litterfall and gross primary production for the native (Thurston) and invaded (Ola'a) sites.

Site	Aboveground Litterfall ( $\text{g biomass m}^{-2} \text{ yr}^{-1}$ )	Aboveground Litterfall ( $\text{g C m}^{-2} \text{ yr}^{-1}$ )	GPP ( $\text{g C m}^{-2} \text{ yr}^{-1}$ )
Thurston Total	179.50	89.8	1121.9
Ola'a Total	288.00	144.0	1800.0
Ola'a Native	237.40	118.7	1483.8
Ola'a Guava	50.60	25.3	316.3

Soil-surface  $\text{CO}_2$  efflux was 38.2 and 81.8% higher at the invaded than the native site in 2014 and 2015, respectively (Table 6. These values agree well with previously published values for similar forests under similar conditions (Litton et al. 2011). In addition, the soil-

surface CO<sub>2</sub> efflux values are in line with site differences in aboveground litterfall (see above). As a fraction of total ecosystem respiration, annual soil-surface CO<sub>2</sub> efflux accounted for 53.4 and 48.6% of ecosystem respiration (Table 6), which is lower than the 70% reported previously for temperate forests.

Table 6. Soil-surface CO<sub>2</sub> efflux (SR) measured at mean annual temperature (SR<sub>MAT</sub>), extrapolated to annual values (SR<sub>Annual</sub>), total ecosystem respiration (R<sub>Ecosystem</sub>) from tower measurements for 2014, and the percentage of R<sub>Ecosystem</sub> accounted for by SR<sub>Annual</sub> for the native (Thurston) and invaded (Ola'a) sites.

Site	Year	SR <sub>MAT</sub> ( $\mu\text{mol CO}_2 \text{ m}^{-2} \text{ s}^{-1}$ )	SR <sub>Annual</sub> ( $\text{g C m}^{-2} \text{ yr}^{-1}$ )	R <sub>Ecosystem</sub> ( $\text{g C m}^{-2} \text{ yr}^{-1}$ )	R <sub>Ecosystem</sub> as SR %
Thurston	2014	2.39	979.0	1834.3	53.4
Thurston	2015	2.24	921.0	-	-
Ola'a	2014	3.40	1353.1	2786.3	48.6
Ola'a	2015	4.27	1674.2	-	-

At the beginning of the study period, AGCD was 43% higher at the native site than the invaded site (Table 7). However, by the end of the study period AGCD of the native stand was only 16% higher than the invaded stand due to the higher growth rates at the invaded site. The invaded stand was found to accumulate carbon at a rate of 359 g C m<sup>-2</sup> yr<sup>-1</sup>, while the native stand accumulated carbon at a rate of 155 g C m<sup>-2</sup> yr<sup>-1</sup>. These results are in agreement with higher GPP and NEE at the invaded site, and are within the range of values reported by Malhi et al. (2004) for coarse wood production in neotropical forest sites (150-550 g C m<sup>-2</sup> yr<sup>-1</sup>). At the invaded site, *P. cattleianum* had considerable spatial variability between study plots (see Table X; a, b), and despite a very slow growth rate of individual stems (average D<sub>BH</sub> increment less than 0.1 cm yr<sup>-1</sup>), the large number of stems allowed the invasive species to contribute 41% to total AGCB on average, while native trees contributed 38%, and tree ferns contributed the remaining 21%. While native trees at the native site gained a similar amount of carbon during the study period, native trees at the invaded site grew significantly faster than at the native site.

LAI at the native site was 4.31 (S.D. = 0.49) and at the invaded site was 5.54 (S.D. = 0.49). This indirect method of estimating leaf area shows that the invaded site had 29% more tissue available for photosynthesis and, therefore, should be expected to have higher rates of both GPP and autotrophic respiration.

### Task 3: Leaf Ecophysiological Characteristics of Native and Non-native Trees at Thurston and Ola'a Field Sites and Implications for Future Changes in Ecosystem Fluxes (see Appendix for more details)

The meteorological and related environmental time series used to scale up leaf level measurements were derived from tower measurements at each site. Measured photosynthetic traits were not consistently different between species. Under wet leaf surface conditions, both species reduced stomatal conductance to 50-60% of the level under the similar light intensities and dry leaf surface conditions. Based on the Leuning et al. (1995) multilayered model, simulated stand-scale gas exchange rates for CO<sub>2</sub> and water vapor did not differ between species. Results suggest that changes in leaf ecophysiological traits alone due to the invasion of *P. cattleianum* would not necessarily alter the gas exchange of the forests in this region, suggesting that differences found at other scales is

caused by other factors, such as differences in leaf area or in the relative contributions of overstory and understory canopies.

Table 7. Above-ground carbon density (AGCD) and increment growth at Native and invaded sites.

	Species	July, 2004 (Mg C ha <sup>-1</sup> )	May, 2016 (Mg C ha <sup>-1</sup> )	Growth (g C m <sup>-2</sup> yr <sup>-1</sup> )
Native Site	native trees	152.0	167.7	134
	<i>M. polymorpha</i>	142.5	157.2	126
	<i>Cibotium</i> spp.	8.4	10.9	21
	Total	160.4	178.5	155
	Native trees include <i>M. polymorpha</i> , <i>Ilex anomala</i> , and <i>Coprosma</i> sp. Based on 4 10 x 10 m tagged plots measured over a ~12 year period. Individuals > 5 cm diameter and all tree ferns ( <i>Cibotium</i> spp. and <i>Sadleria</i> sp.)			
Invaded Site	(a) Species	July, 2006 (Mg C ha <sup>-1</sup> )	May, 2016 (Mg C ha <sup>-1</sup> )	Growth (g C m <sup>-2</sup> yr <sup>-1</sup> )
	native trees	41.9	57.8	162
	<i>M. polymorpha</i>	35.2	49.6	147
	<i>P. cattleianum</i>	46.3	58.4	123
	<i>Cibotium</i> spp.	23.3	29.5	063
	Total	111.4	145.7	349
	Based on 4 10x10 m tagged plots re-measured after a ~10 year period			
	(b) Species	July, 2004 (Mg C ha <sup>-1</sup> )	May, 2016 (Mg C ha <sup>-1</sup> )	Growth (g C m <sup>-2</sup> yr <sup>-1</sup> )
	native trees	49.0	59.5	89
	<i>M. polymorpha</i>	11.3	22.3	93
	<i>P. cattleianum</i>	51.7	74.8	195
	<i>Cibotium</i> spp.	25.9	37.4	97
	Total	126.6	171.7	381
	Based on 2 10x10 m tagged plots re-measured after a ~12 year period For (a) and (b), native trees include <i>M. polymorpha</i> , <i>I. anomala</i> , and <i>C. trigynum</i> Individuals > 5 cm diameter, <i>P. cattleianum</i> > 2 cm diameter, and all tree ferns ( <i>Cibotium</i> spp.)			

The multilayer model showed the strong dependence of gas exchange rates on daily PAR, suggesting that future increase in PAR would increase both water vapor and CO<sub>2</sub> fluxes. Transpiration rates depended on the daily mean relative humidity, rather than VPD, and explained the scatter of transpiration rates – PAR relationship. These sites with different dominant species had similar leaf-level ecophysiological traits, and therefore, the response in net photosynthesis and transpiration rates were identical.

Task 4: Implementation of the Community Land Model to Simulate Present and Future Ecosystem Fluxes at the Thurston and Ola'a Study Sites (see Appendix for more details)

The results of the CLM simulations of net ecosystem carbon exchange (NEE), gross primary production (GPP), and latent energy flux (LE, evapotranspiration) are give for Thurston in Table 8 and Ola'a in Table 9.

Table 8. Mean annual simulated fluxes at Thurston in the observational period and under future scenarios.

Scenario	NEE (gC m <sup>2</sup> yr <sup>-1</sup> )			GPP (gC m <sup>2</sup> yr <sup>-1</sup> )			LE (W m <sup>2</sup> )		
SLA <sub>0</sub>	default	Sen1	Sen2	default	Sen1	Sen2	default	Sen1	Sen2
Present	-194.55	-212.74	-71.68	2739.9	2848.3	1776.9	56.77	58.01	48.11
Scenario 1	-145.99	-169.26	-39.00	2939.1	3065.7	1926.3	60.64	61.98	51.05
Scenario 2	-191.20	-209.10	-69.03	2905.6	3003.7	1936.6	59.58	60.90	49.86

Table 9. Mean annual simulated fluxes at Ola'a in the observational period and under future scenarios.

Scenario	NEE (gC m <sup>2</sup> yr <sup>-1</sup> )			GPP (gC m <sup>2</sup> yr <sup>-1</sup> )			LE (W m <sup>2</sup> )		
SLA <sub>0</sub>	default	Sen1	Sen2	default	Sen1	Sen2	default	Sen1	Sen2
Present	-148.22	-91.78	-59.28	2685.7	2168.2	1771.1	54.10	49.50	46.52
Scenario 1	-68.53	-28.17	-18.24	2819.1	2284.0	1890.2	55.64	50.73	47.62
Scenario 1	-114.45	-59.61	-41.17	2835.5	2298.0	1900.8	55.36	50.21	46.85

## 7. ANALYSIS AND FINDINGS:

*Present-day Evapotranspiration.* Based on nine years of tower measurements (Task 1), present day evapotranspiration (ET) was found to be higher at Ola'a than Thurston, and much higher when normalized for available energy. However, analysis of leaf-level measurements (Task 3) did not find any difference between the transpiration rates of 'ōhi'a and strawberry guava. Based on the leaf level analysis, the higher stand level ET at Ola'a is not the result of higher transpiration by strawberry guava.

*Present-day C flux.* Tower measurements (Task 1) indicate that photosynthesis (GPP) is 35% higher at Ola'a than Thurston, while respiration ( $R_{eco}$ ) is 48% higher at Ola'a than Thurston. As a result, carbon accumulation (NEE) is 19% lower at Ola'a than at Thurston. Measurements of soil respiration (Task 2), a major component of  $R_{eco}$ , give rates about 59% higher on average at Ola'a than at Thurston, in general agreement with the tower measurements. Biometric measurments of above ground carbon storage (Task 2) suggest that carbon storage is increasing at Ola'a at a rate more than double that of Thurston. While this result differs from that obtained with the tower measurements, the rates of aboveground C accumulation are of a similar magnitude to these found in Task 1.

*Sensitivity of ET to Environmental Conditions.* Based on tower measurements (Task 1), ET was most sensitive to net radiation ( $R_{net}$ ), vapor pressure deficit (VPD), and canopy wetness fraction (FW) at both sites. Similarly, the leaf-level measurements (Task 3) showed that transpiration was sensitive to photosynthetically-active radiation (PAR; highly correlated with  $R_{net}$ ), relative humidity (RH; highly negatively correlated with VPD), and leaf wetness.

*Sensitivity of C Fluxes to Environmental Conditions.* Based on tower measurements (Task 1), net ecosystem exchange (NEE) was most sensitive to PAR and VPD. Leaf-level measurements (Task 3) showed that photosynthesis is sensitive to PAR and leaf wetness.

*Projected Changes in ET.* Based on statistical analysis of tower measurements (Task 1), the projected changes in climate are expected to increase in ET at both sites (+10 to 12 % wet season and +13 to 14% dry season at Thurston; +19 to 20% wet season and +15 to 18% dry season at Ola'a). Transpiration (Task 3) is projected to increase by a maximum of 5.6% at Thurston and 7.8% at Ola'a. Experimental runs of the Community Land Model (CLM; Task 4) indicate that ET will increase by 4 to 7% at Thurston and by 1 to 3% at Ola'a.

*Projected Changes in C Fluxes.* Statistical analysis of tower measurements (Task 1) project that NEE at Thurston will decrease to 3 to 9% in the wet season and increase change by -1 to +5% in the dry season. NEE at Ola'a is projected to decrease by 17 to 24% in the wet season and by 8 to 14% in the dry season. Analysis of leaf-level measurements that the maximum changes in photosynthesis will be increases of 1.4% at Thurston and 1.6% at Ola'a. CLM results (Task 4) project NEE decreases of 2 to 46% at Thurston and 31 to 69% at Ola'a.

## 8. CONCLUSIONS AND RECOMMENDATIONS:

Synthesizing the findings derived from the different approaches used in this study, we draw the following conclusions:

- a) Evapotranspiration (ET) is higher at the non-native forest site (Ola'a) compared with the native forest site (Thurston). This difference is enhanced when ET is controlled by available energy. However, leaf-level measurements do not show any significant differences between the gas exchange characteristics of the principal native (*M. polymorpha*) and non-native (*P. cattleianum*) tree species. If the leaf-level results are correct, the significant stand level differences in ET apparently do not result from greater transpiration by *P. cattleianum*, but instead are the result of differences in contributions of species other than *P. cattleianum*, or some combination of the effects of differences in stand structure, climate, soil depth, soil physical characteristics, or soil nutrient availability.
- b) Gross primary production (GPP) is significantly greater at the non-native forest site (Ola'a) compared with the native forest site (Thurston). However, the leaf-level finding of no significant differences between the gas exchange characteristics of *M. polymorpha* and *P. cattleianum* suggest that the GPP difference does not result from higher photosynthesis by *P. cattleianum*. We are left to question what causes GPP to be higher at Ola'a.
- c) Ecosystem respiration ( $R_{eco}$ ) is much higher at Ola'a than at Thurston. The site difference is explained in part by the higher temperature at the slightly lower elevation Ola'a site. However, the large  $R_{eco}$  difference cannot be fully explained by temperature. It is likely that species-specific contrasts in rates of decomposition contribute to this effect.
- d) Net ecosystem exchange (NEE) is positive at both sites. Based on tower measurements, Thurston is accumulating carbon faster than Ola'a. Biometric measurements of aboveground C storage show that Ola'a is growing more than twice as fast as Thurston. It is not clear which of these estimates is correct.
- e) Analysis of ET sensitivity to environmental variables indicates that, at both sites, net radiation ( $R_{net}$ ) is the dominant control with additional influences from atmospheric dryness (vapor pressure deficit, VPD) and canopy wetness fraction (FW). It is interesting to note that ET was found to be insensitive to variations in temperature and soil moisture.
- f) NEE was found to be most sensitive to variations in photosynthetically-active radiation (PAR) and VPD at both sites. GPP is driven by PAR and temperature and  $R_{eco}$  varies with temperature. The opposite effects of temperature on GPP and  $R_{eco}$

- cancel and leave NEE with no sensitive to changes in temperature.
- g) Based on the end-of-century climate scenarios derived from statistical downscaling, ET is projected to increase by an average of around 12% at Thurston and 18% at Ola'a based on analysis of tower measurements. Other approaches gave smaller increases.
  - h) Projections of changes in carbon fluxes due to climate change resulted in a small average decrease in NEE at Thurston and a somewhat larger decrease at Ola'a. Using the Community Land Model, much larger decreases in carbon accumulation rates were projected.

Overall, these findings point to significant climate change effects on ecosystem function and related ecosystem services for both study sites. Site differences in current fluxes are significant, but the causes of the differences are not clear. The non-native site differences in several ways other than the presence of the invasive tree *P. cattleianum*, and those other differences might or might not be an effect of the invasion.

## **9. MANAGEMENT APPLICATIONS AND PRODUCTS:**

While it might not be possible to draw firm conclusions regarding the differential effects of climate change on native vs. non-native ecosystems in Hawai'i, it is possible to conclude that climate change will have significant effects on both ecosystems. These changes will include increases in evapotranspiration in areas where radiation increases accompany a decrease in rainfall. Increased evapotranspiration will exacerbate the effects of decreased rainfall in areas where it occurs. Climate change is also projected to have negative effects on growth. This effect appears to be larger at our non-native forest site, although it is not clear that this site difference is caused by the presence of the non-native tree *P. cattleianum*. The implications of reduced forest growth rates should be explored with further research. Possible effects are decreases in native forest vigor and resistance to disease and invasion.

## **10. OUTREACH:**

### *Outreach:*

- Presented to and interacted with a large group of resource managers and practitioners at the 8<sup>th</sup> Annual Dryland Forest Symposium, Kailua-Kona, Hawai'i, February 2014.
- Gave presentation and participated in discussion at Three Mountain Alliance meeting, Hilo, Hawai'i (Jun 2014).
- Gave a presentation and participated in discussions with community members at workshop organized by Ka Honua Momona on Moloka'i (Sep 2014)
- Continued informal communication with resource managers, including CWRM staff, HAVO Resources Management staff, and HALE Resources Management staff (Oct-Dec 2014).
- Continued informal communication with resource managers, including CWRM staff, HAVO Resources Management staff, and HALE Resources Management staff (Jan-Mar 2015).
- Gave a presentation before a workshop convened by the Maui Department of Water Supply on the role of vegetation and vegetation change in controlling water processes on Maui (Mar 2015).
- Gave a presentation and participated in discussions with community members at workshop organized by Ka Honua Momona on Moloka'i (Apr 2015)
- Gave a presentation and participated in discussions with community members at workshop organized by Ka Honua Momona on Moloka'i (Jul 2016)

*Publications and Presentations:*

- Giambelluca, T.W. 2014. Climate change and Hawai'i's forests. 8<sup>th</sup> Annual Dryland Forest Symposium, Kailua-Kona, Hawai'i, February 2014. (Invited)
- Giambelluca, T.W. 2014. Understanding response of native and non-native forests to climate variability and change to support resources management in Hawai'i. Three Mountain Alliance meeting, Hilo, Hawai'i, June 2014.
- Giambelluca, T.W., Elison Timm, O., Diaz, H., Takahashi, M., Frazier, A., and Longman, R. 2014. Climate variability and change in Hawai'i. Moloka'i Climate Change Collaboration Project: Workshop 1, Ka Honua Momona, Kawela, Moloka'i, Hawai'i, September 2014. (Invited)
- Giambelluca, T.W., Ostertag, B., Litton, C., Fortini, L., Huang, M., Asner, G., and Miyazawa, Y. 2015, Understanding the response of native and non-native forests to climate variability and change to support resource management in Hawai'i. 2015 Climate Science Symposium, Pacific Islands Climate Science Center, Honolulu, February 2015.
- Giambelluca, T., Mudd, R., Huang, M., Miyazawa, Y., Nullet, M., DeLay, J., Asner, G., Martin, R., Ostertag, R., Litton, C. 2015. Invasive non-native trees in Hawaiian forests could increase negative impacts of climate change on water resources. Abstract H24B-04 presented at the American Geophysical Union Fall Meeting, San Francisco, December 2015.

*Planned Publications and Presentations:*

- Paper, "Light availability controls ecosystem fluxes in native and non-native tropical montane wet forests in Hawai'i" to be presented at the 2016 meeting of the American Geophysical Union, Dec 2016 (abstract submitted).
- Scientific paper on gas exchange characteristics of the principal tree species at native and non-native forest sites in Hawai'i (draft complete).
- Scientific paper on native Hawaiian forest carbon exchange, based on the tower observations and analysis at Thurston (draft partially complete).
- Scientific paper on differences in forest carbon exchange at native and non-native forest sites in Hawai'i, based on the tower observations and analysis (currently in preparation).
- Scientific paper on the evapotranspiration at native and non-native forest sites in Hawai'i (currently in preparation).
- Scientific paper on growth rates based on biometric measurements and soil respiration at native and non-native forest sites in Hawai'i (currently in preparation).
- Scientific paper on the application of the Community Land Model to simulate and project future changes in ecosystem fluxes at native and non-native forest sites in Hawai'i (currently in preparation).
- PhD dissertation by Ryan Mudd on ecosystem carbon dynamics of native forests, non-native forests, and non-native tree plantations.

## **APPENDIX**

**to**

### **Project Final Report**

#### **Understanding the response of native and non-native forests to climate variability and change to support resource management in Hawai‘i**

1 October 2016

Thomas Giambelluca  
Maoyi Huang  
Creighton Litton  
Rebecca Ostertag  
Gregory Asner  
Yoshiyuki Miyazawa  
Lucas Fortini  
Yi Xu  
Roberta Martin  
Ryan Mudd

With contributions from

Christian Giardina  
Michael Nullet

**Task 1: Measurement and Analysis of Meteorological and Eddy Covariance data from Native and Non-native Forest Sites in Hawai‘i Volcanoes National Park**

**Task 2: Validation of Flux Tower Observations with Biometric Measurements**

**Task 3: Leaf Ecophysiological Characteristics of Native and Non-native Trees at Thurston and Ola‘a Field Sites and Implications for Future Changes in Ecosystem Fluxes**

**Task 4: Implementation of the Community Land Model to Simulate Present and Future Ecosystem Fluxes at the Thurston and Ola‘a Study Sites**

## **Task 1: Measurement and Analysis of Meteorological and Eddy Covariance data from Native and Non-native Forest Sites in Hawai'i Volcanoes National Park**

### **PURPOSE AND OBJECTIVES:**

Fluxes of water vapor, carbon dioxide, and energy between forest ecosystems and the atmosphere are fundamentally important to ecosystem health and survival, water cycling, carbon storage, and competition among plant species. Flux of water vapor, or evapotranspiration, is a major component of the hydrological cycle and a dominant control on environmental water flows (streamflow and groundwater recharge) and local and regional climate. Carbon dioxide flux describes the dynamics of photosynthesis and respiration, the uptake and release of carbon by terrestrial ecosystems, with important consequences for plant growth and survival and the sequestration of carbon in the biosphere. Energy fluxes, including radiation exchange, and sensible and latent energy transfer between the ecosystem and the atmosphere, strongly controls local climate.

To address the overall project objective, to determine the possible effects of future climate change on native and non-native forest ecosystems in Hawai'i, the tasks focuses on measurement and analysis of ecosystem fluxes and related environmental variables at two field sites in Hawai'i Volcanoes National Park. Using the eddy covariance approach, and taking advantage of the existing field infrastructure and previously obtained data, monitoring of ecosystem fluxes was extended to approximately nine years at each site.

### **ORGANIZATION AND APPROACH:**

#### *Climate Change Scenario*

To estimate the effects of projected climate change on ecosystem fluxes for the two study sites in this project, we examined the downscaled climate projections of Ellison Timm et al. (2015) for rainfall and Ellison Timm and Fortini (2016) for temperature. We selected the projects for late century (2071-2100) and for the RCP8.5 emissions scenario. Both the rainfall and temperature projections were derived by statistical downscaling of CMIP5 global model projections. Climate shifts used in our analysis do not represent the precise values predicted at either of the study sites, but rather the range of projected changes for areas similar to the study sites. For this test, only statistical downscaling results are used to develop the scenarios. It should be noted that projections based on dynamical downscaling (Zhang et al. 2012) indicate significant increases in seasonal rainfall for the same areas, contrasting with those used in this study.

The Ellison Timm and Fortini (2016) temperature projection gives a statewide mean air temperature change of +3.5°C. Their projection shows enhancement of temperature change with elevation. The areas represented by the study sites are in the middle elevation range. Hence, use of the statewide average change is reasonable.

The Ellison Timm et al. (2015) rainfall projections show modest rainfall increases

Wet Season (Nov-Apr) Precipitation Change: 0% to -20%

Dry Season (May-Oct) Precipitation Change: -30% to -50%

Changes in solar radiation (PAR) and relative humidity (RH) were estimated by relating present-day monthly variations in PAR and RH to variations in RF at Thurston Tower. The resulting sensitivities are very low for RH. The association between Solar radiation and Rainfall is greater,

e.g., for a 50% decrease in RF, PAR would increase by 4.8%. The scenarios used in this study are given in Table 1.

Table 1. Climate scenarios selected for analysis in this project, derived from statistical downscaling projections of Elison Timm et al. (2015) and Elison Timm and Fortini (2016).

Scenario 1		Change from Present		
	T	RF	RH	Solar
Wet Season	+3.5°C	0%	0%	0%
Dry Season	+3.5°C	-30%	0%	+2.9%

Scenario 2		Change from Present		
	T	RF	RH	Solar
Wet Season	+3.5°C	-20%	0%	+1.9%
Dry Season	+3.5°C	-50%	0%	+4.8%

### Energy Balance Framework

The vertical exchanges of energy for a land surface can be described as

$$R_{\text{net}} - LE - H - G - S_{\text{biomass}} - S_{\text{air}} = 0 \quad (1)$$

where  $R_{\text{net}}$  = net radiation,  $LE$  = latent heat flux to the atmosphere,  $H$  = sensible heat flux to the atmosphere,  $G$  = sensible heat flux to the soil,  $S_{\text{biomass}}$  = change in stored sensible energy in the biomass,  $S_{\text{air}}$  = change in stored sensible and latent energy in the air between the eddy covariance sensors and the ground, and  $Q$  = the sum of all other sources and sinks (units:  $\text{W m}^{-2}$ ). At each of the two field sites,  $R_{\text{net}}$ ,  $LE$ ,  $H$ ,  $G$  were measured, and  $S_{\text{biomass}}$  and  $S_{\text{air}}$  were estimated from measurements of air temperature and humidity and biomass temperature.  $LE$  is the energy equivalent of evapotranspiration ( $ET$ ) and can be readily converted into  $ET$ . For the purpose of discussion about temporal variability and site differences in  $ET$ ,  $LE$  will be used.

### Field Measurements

Operation of two existing flux towers, equipped with state-of-the-art eddy covariance sensors and related meteorological instruments and data loggers to measure the vertical exchanges of energy, water, and carbon between the ecosystem and the atmosphere (Giambelluca et al, 2009) was continued for most of the project period. Eddy covariance measurements provide 30-minute-resolution flux data, which, together with relevant micrometeorological time series, allow for quantification of the varied and interacting controls on energy, water vapor, and  $\text{CO}_2$  fluxes.

Study sites. Two established field sites, both located within Hawai'i Volcanoes National Park (HAVO) on Hawai'i Island, were used for this study, representing tropical montane wet native and non-native forests in Hawai'i. The upper canopy at the native forest site is dominated by *Metrosideros polymorpha* and the mid-canopy by the native tree fern *Cibotium glaucum*. The invaded site, where the invasive tree *Psidium cattleianum* has encroached, is about 7.5 km north-northeast of the native site, and has a slightly wetter climate (Table 2). Detailed descriptions of the sites are given by Giambelluca et al. (2009), Takahashi et al. (2011), and Mudd (2012).

Micrometeorological instrumentation. Measurement of energy, water vapor, and carbon dioxide exchange, and related micrometeorological variables began in February 2005 at the native site and February 2006 at the non-native site. A three-dimensional sonic anemometer (CSAT3,

Campbell Scientific, Logan, UT, USA) and an open-path infrared gas analyzer (LI-7500, Licor, Lincoln, NE, USA) installed 6-8 m above the canopy at each site, are being used to estimate turbulent energy and mass fluxes using the eddy covariance method. A complete list of tower instrumentation at the native site is given by Giambelluca et al. (2009). Instrument configuration is virtually identical at the non-native site.

Table 2. Site characteristics of the native and non-native forest study sites. (Takahashi et al. 2011).

Site and Meteorological Properties	Native Site	Non-native Site
Elevation (m)	1201	1029
Mean annual precipitation (mm)	2734	3233
Mean annual temperature (°C)	14.6	15.2
Mean annual wind speed (m s <sup>-1</sup> )	4.4	2.5
Mean annual net radiation (W m <sup>-2</sup> )	147	132

#### *Analysis of Ecosystem Water Vapor, Carbon Dioxide, and Energy Fluxes*

The key measurements needed for the eddy covariance (EC) technique are obtained using a three-dimensional sonic anemometer (model CSAT3, Campbell Scientific, Logan, UT, USA) and an open-path infrared gas analyzer (IRGA, model LI-7500, LiCor, Lincoln, NE, USA) each installed at a height of several meters above the forest canopy. These measurements are needed to estimate latent and sensible energy flux and CO<sub>2</sub> flux. By estimating all energy balance components we are able to assess the reliability of flux measurements by checking energy balance closure.

The following summary of the eddy covariance flux analysis is quoted from Giambelluca et al. (2009):

Before calculating fluxes, raw 10-Hz data were filtered to remove spikes, and to screen out out-of-range values for each variable, high-moment statistics were evaluated to detect possible sensor or logger malfunctions, and discontinuities were detected and removed. For each 30-min period, means and standard deviations of wind ( $U_x$ ,  $U_y$ ,  $U_z$ ) and sonic temperature ( $T_{\text{sonic}}$ ) from the CSAT3, water vapor ( $H_2O$ ), carbon dioxide concentration ( $CO_2$ ), and air pressure ( $P$ ) from the LI-7500, and air temperature ( $T_{\text{air}}$ ) and vapor pressure ( $e$ ; derived from  $T_{\text{air}}$  and  $RH$ ) from the HMP45C were computed after removing out-of-range data points. For each variable  $x$ , data points ( $x_i$ ) for which  $x_i > \bar{x} + 6\sigma$  or  $x_i < \bar{x} - 6\sigma$  were identified as spikes and replaced with  $\bar{x}$ . Means ( $\bar{x}$ ) and standard deviations ( $\sigma$ ) were recalculated after removing spikes. The coordinate system for the three dimensional wind velocity variables was rotated, first around the  $z$ -axis, then around the  $y$ -axis, according to the method of [Tanner and Thurtell \(1969\)](#) (also see [Wilczak et al., 2001](#)), so that the mean wind direction in each 30-min period lies along the  $x$  axis and the mean vertical velocity was forced to zero. LE, H, and carbon dioxide flux ( $FCO_2$ ) were computed using the covariances of the rotated 10-Hz vertical wind velocity with the 10-Hz water vapor concentration, sonic temperature, and carbon dioxide concentration, respectively. Fluxes were corrected for density effects ([Webb et al., 1980](#)). Using sample 30-min intervals during each month of the study period, including early morning, midmorning, afternoon, evening, and late night periods, the water vapor spectrum and the cospectra of water vapor and vertical wind velocity were evaluated using the method of [Högström et al. \(1989\)](#) (also see [Goulden et al., 1996](#)). Spectral losses were found to be negligible, ranging from 0 to 1.5% for water vapor

flux, with typical losses near 0.5–0.6%. No corrections were applied for spectral loss. Our code to analyze the EC data was based in part on that of Noormets et al. (2007) and Baldocchi et al. (1988).

The 30-min fluxes were filtered so that periods were included only if (a) wind direction was 0–110° or 315–360°, which excludes periods with wind trajectories disturbed by tower and sensor interference and trajectories over heterogeneous land cover and/or rough terrain; (b) friction velocity was greater than a threshold of 0.22 m s<sup>-1</sup> (determined based on the method described by Saleska et al. (2003) and Miller et al. (2004)); (c) energy closure error (ECE), defined as

$$ECE = R_{net} - G - LE - H \quad (2)$$

was between -200 and 400 W m<sup>-2</sup>. For statistical analysis involving comparison among energy terms, periods were excluded if any energy term was missing. Both the sonic anemometer and the IRGA output diagnostic indices, “csat warning” and “agc”, respectively. The csat-warnings are triggered by detection of abrupt changes in sonic temperature, poor signal lock, sonic signal higher or lower than expected amplitude range, all of which can be caused by an obstruction in the anemometer. The agc variable indicates the optical clarity of the sensor window and responds to the presence of water droplets (LI-COR Inc., 2004). We found these variables to be valuable indicators of wet sensor conditions. Both instruments perform poorly when the sensing surfaces are wet. A csat-warnings value >0 (for the sonic anemometer) and an agc value >50, were found to be consistent indicators of sensor wetting. Thirty-minute periods were therefore excluded when either or both of these variables exceeded their respective thresholds. Lastly, limited manual screening of outlier points was done for each of the 30-min flux time series.

### *Energy Closure Adjustment*

With independent measurements or estimates of all significant terms in the energy balance equation, energy balance closure can be evaluated by comparing the sum of estimated turbulent fluxes (LE + H) to the available energy ( $R_{net} - G - S_{biomass} - S_{air}$ ). Assuming no significant horizontal energy exchange, these two sums should be equal. However, experience at other eddy covariance sites has shown that measured LE + H is generally lower than  $R_{net} - G - S_{biomass} - S_{air}$ . For example, energy closure error was in the 20-30% range at most tropical forest flux tower sites in the Large-Scale Biosphere Atmosphere Experiment (LBA) in Amazonia, (Fisher et al., 2009). It is sometimes assumed that LE and H are both underestimated and for similar reasons, such that the ratio of H to LE (Bowen ratio) can be considered accurate. Some researchers advocate adjusting H and LE using the Bowen ratio closure method (Twine et al. 2000), in which LE and H are each adjusted by a factor of the inverse of the energy closure ratio to force energy closure. In this study, we report latent energy flux as both unadjusted and adjusted values. To adjust LE, the monthly energy closure ratio (ECR) time series was calculated as:

$$ECR = \frac{LE + H}{R_{net} - G - S_{biomass} - S_{air}} \quad (3)$$

where all terms are means of individual months throughout the period of record. This time series was used to adjust the 30-min values of LE and H by a factor of ECR<sup>-1</sup>.

### *Gap-Filling LE and CO2 Flux Time Series*

Because of frequency sensor wetting, eddy covariance data have a large number of missing data periods at both sites. To obtain representative mean annual cycles of these fluxes, and for estimate of mean monthly fluxes, it is important to fill as many gaps as possible using accurate estimation techniques. Failure to fill gaps will result in over estimation of LE (evapotranspiration) because data gaps coincide with wet, cloudy, humid periods when LE tends to be lower than average. For CO<sub>2</sub> exchange, gaps occur mainly during nighttime periods when flux is equivalent to ecosystem respiration. It is important to accurately estimate nighttime CO<sub>2</sub> flux in order to obtain reliable estimates of Net Ecosystem Exchange (NEE). The steps used in testing and implementing LE and CO<sub>2</sub> Flux gap filling are listed below.

#### **LE Gap Filling**

1. Use Mudd (2012) analysis to get relationship between Qsum and Rn and use it to estimate 30-min Rn-Qsum for whole record (Qsum = sum of soil heat flux, biomass heat flux, sensible heat storage in air layer, and latent heat storage in air layer).
2. Get mean energy closure ratio  $LE+h/Rn-Qsum$  for each month of record
3. Used the energy closure ratio of a given month to calculate adjusted LE and h ( $LE\_adj(i,j) = LE(i,j)/ECR(j)$  and  $h\_adj(i,j) = h(i,k)/ECR(j)$ ) for each 30-min period with data (i: subscript for 30-min period; j: subscript for month)
4. Calculate 30-min Ga as  $u \cdot star^2 / u$
5. Ga-fill Ga using regression with u; scale slope and intercept as a function of PAR; scale differently for day and night (based on PAR thresholds)
6. Calculate Gs and Gs\_adj using Penman-Monteith and tower flux measurements
7. Filter Gs and Gs\_adj to remove values less than -10 and greater than 75
8. Identify and separate periods with dry canopy based on LW1, LW2, and LW3. Dry periods defined as periods when all three LW sensors values are less than or equal to 2 mV.
9. Get mean diurnal cycles of Gs, Gs\_adj, Gs\_dry, Gs\_adj\_dry (long-term January mean diurnal cycle, long-term February mean diurnal cycle, etc.)
10. Focus on Dry period values.
11. Use only Daytime values (timestamps 0700-1800) [includes period 0630-1800].
12. Arbitrarily assign nighttime value of 1 for Gs\_dry and Gs\_adj\_dry
13. Smooth the diurnal cycles using 3-point, centered moving average
14. Calculate midday means of Gs\_dry and Gs\_adj\_dry (timestamps 0930-1400) [includes period 0900-1400]
15. Normalize the smoothed 30-min mean diurnal cycles of Gs-dry and Gs-adj\_dry for each of the 12 long-term mean months by dividing by each month's mean midday value
16. Get the all-month mean diurnal cycle of the normalized, smoothed Gs\_dry and Gs\_adj\_dry: T(i)
17. Seasonal analysis:
  - a. For each 3-mo season of each year (DJF, MAM, JJA, and SON; DJF associated with Jan year):
  - b. Calculate mean midday Gs\_dry and Gs\_adj\_dry (timestamps 0930-1400) [includes period 0900-1400]
  - c. Get mean Gs\_dry and Gs\_adj\_dry overall all years for each season
  - d. Normalize the individual seasonal means by dividing by the long-term seasonal mean
  - e. To get monthly midday factor, center the seasonal estimate and interpolate
18. Estimate 30-min Gs as  $Gs = MDM * Midday\_factor$

## Carbon Flux Gap Filling

1. Nighttime: Need to gap fill nighttime because of general data scarcity
2. Goal here is to estimate Reco throughout the study period
3. Use nighttime  $\text{co}_2$ \_flux\_plus\_dSCO<sub>2</sub> to estimate Reco or develop a model for simulating Reco
4. Daytime: Need to gap fill at basic 30-min interval to reduce the biasing effect of removing wet canopy periods
5. Calculate Reco for daytime periods using the model developed from nighttime values
6. Calculate GPP for daytime periods as  $\text{co}_2$ \_flux\_plus\_dSCO<sub>2</sub> minus Reco
7. Regress GPP = f(PAR) for each month
8. Gap fill GPP
9. Daytime Gap fill NEE as gap-filled GPP + gap-filled Reco
10. Methods tested for Reco model:
  - a. NEE Light response curve method
  - b. Screening nighttime values of  $\text{co}_2$  flux based on different  $u^*$  thresholds
  - c. Nighttime NEE vs. T
  - d. Van Gorsel approach
11. Van Gorsel et al. (see Ola'a Ola'a \_Van Gorsel.xlsx)
  - a. Use only the period with CO<sub>2</sub> profiler data (4/20/2013 - 8/14/2014)
  - b. Take data only for evenings with at least 4 30-min  $\text{co}_2$ \_flux+SCO<sub>2</sub> values between 19:00 and 24:00 (inclusive)
  - c. Take the highest measured  $\text{co}_2$ \_flux+SCO<sub>2</sub> value for each sample evening as a true Reco value
  - d. Extract the air temperature for the same time interval as the selected  $\text{co}_2$ \_flux+SCO<sub>2</sub> value
  - e. Regress  $\text{co}_2$ \_flux+SCO<sub>2</sub> = f(Temp) using linear, exponential, and power functions
12. Regression Results:
  - a. Linear
    - i. `lm(formula = van_gorsel_N4 ~ T_hmp)`
    - ii. Residuals:
    - iii. Min 1Q Median 3Q Max
    - iv. -5.5930 -1.7592 -0.6021 0.8728 9.6735
    - v. Coefficients:
    - vi. Estimate Std. Error t value Pr(>|t|)
    - vii. (Intercept) -0.9745 2.3589 -0.413 0.680063
    - viii. T\_hmp 0.5446 0.1560 3.492 0.000621 \*\*
    - ix. ---
    - x. Signif. codes: 0 '\*\*\*' 0.001 '\*\*' 0.01 '\*' 0.05 '.' 0.1 ' ' 1
    - xi. Residual standard error: 2.77 on 160 degrees of freedom
    - xii. Multiple R-squared: 0.0708, Adjusted R-squared: 0.065
    - xiii. F-statistic: 12.19 on 1 and 160 DF, p-value: 0.0006206
  - b. Power
    - i. `lm(formula = logy ~ logs)`
    - ii. Residuals:
    - iii. Min 1Q Median 3Q Max
    - iv. -1.15437 -0.22437 -0.02272 0.18950 0.85627
    - v. Coefficients:
    - vi. Estimate Std. Error t value Pr(>|t|)
    - vii. (Intercept) -1.0589 0.8022 -1.320 0.188679
    - viii. logx 1.0952 0.2961 3.699 0.000297 \*\*\*
    - ix. —
    - x. Signif. codes: 0 '\*\*\*' 0.001 '\*\*' 0.01 '\*' 0.05 '.' 0.1 ' ' 1
    - xi. Residual standard error: 0.3625 on 160 degrees of freedom

- xii. Multiple R-squared: 0.07878, Adjusted R-squared: 0.07302
- xiii. F-statistic: 13.68 on 1 and 160 DF, p-value: 0.0002971
- c. Exponential
  - i.  $\text{lm}(\text{formula} = \log y \sim T\_hmp)$
  - ii. Residuals:
  - iii. Min 1Q Median 3Q Max
  - iv. -1.15538 -0.22571 -0.02043 0.18895 0.85281
  - v. Coefficients:
  - vi. Estimate Std. Error t value Pr(>|t|)
  - vii. (Intercept) 0.78532 0.30906 2.541 0.01200\*
  - viii. T\_hmp 0.07444 0.02043 3.643 0.000364 \*\*\*
  - ix. ---
  - x. Signif. codes: 0 '\*\*\*' 0.001 '\*\*' 0.01 '\*' 0.05 '.' 0.1 ' ' 1
  - xi. Residual standard error: 0.3629 on 160 degrees of freedom
  - xii. Multiple R-squared: 0.07659, Adjusted R-squared: 0.07082
  - xiii. F-statistic: 13.27 on 1 and 160 DF, p-value: 0.0003639
- 13. Preliminary Conclusions:
  - a. While the power function worked best, the exponent was <1 giving a physically unreasonable result.
  - b. The exponential model is tentatively selected for estimating R\_eco:  $\text{Reco} = a \cdot \exp(b \cdot T_{\text{air}})$
  - c.  $a = \exp(0.78532) = 2.193109$
  - d.  $b = 0.07444$
  - e.  $\text{Reco} = 2.193109 \cdot \exp(0.07444 \cdot T_{\text{air}})$
- 14. Gap filling nighttime NEE
- 15. See spreadsheet: Ola'a\_PAR\_T\_VPD\_NEE.xlsx
- 16. Start with Screened\_CO2\_plus\_dSCO2
- 17. Get Reco calculated as a function of temperature:  $\text{Reco} = 2.193109 \cdot \exp(0.07444 \cdot T_{\text{air}})$
- 18. Replace all nighttime values of NEE (Screened\_CO2\_plus\_dSCO2) with Reco as an exp. function of T
- 19. Reco Adjustment: If NEE minus Reco > 0, then Reco was reset to equal NEE. A total of 138 30-min R\_eco values were adjusted in this step.

## PROJECT RESULTS:

The flux estimates derived from nine years of tower measurements at the two field sites provide the first multiyear, high temporal resolution record of stand-level ecosystem fluxes in Hawai'i. These measurements and the accompanying meteorological measurements provide valuable information relevant to a wide range of problems. These data are central to addressing the objective of this project by providing (1) the basis for direct statistical analysis of the sensitivity of ecosystem fluxes to climate variability, (2) data used to scale up leaf level measurements of ecosystem fluxes, and (3) and providing both forcing data and optimization data for the use of the Community Land Model to conduct computer model experiments to simulate present and future fluxes.

### *Energy Closure*

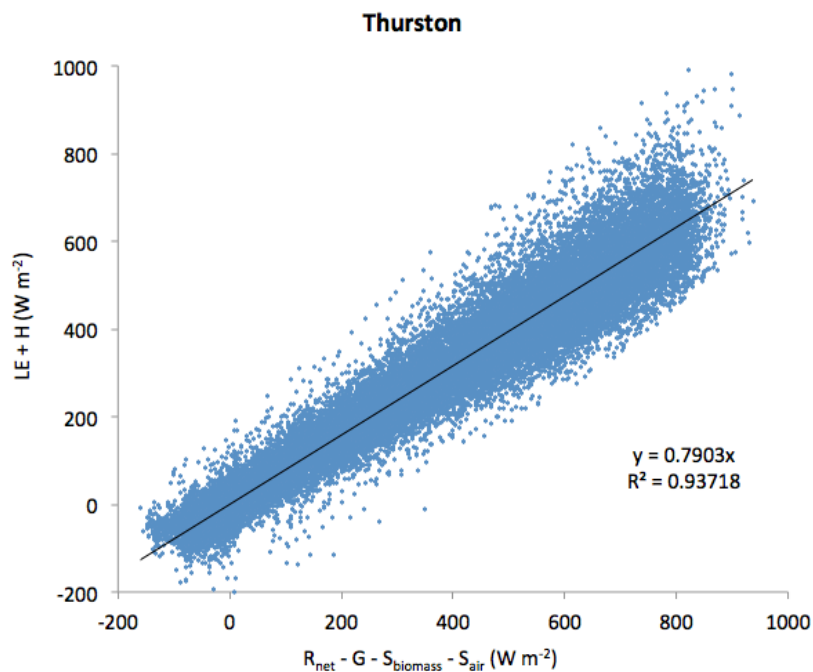
Comparison of the sum of turbulent energy fluxes ( $LE + H$ ) with available energy ( $R_{net} - G - S_{biomass} - S_{air}$ ) provides a check on the quality of the eddy covariance estimates and provides a method for adjusting the data to achieve energy closure. The scatterplots of  $LE + H$  vs.  $R_{net} - G - S_{biomass} - S_{air}$  show excellent agreement between turbulent and available energy fluxes for both sites. The average energy closure is about 79 and 99% at Thurston and Ola'a, respectively, well within the range found for flux tower sites globally. Figure 2 shows the monthly time series of ECR, which was used to adjust  $LE$  and  $H$ .

### *Evapotranspiration*

The results of the  $ET$  estimates derived from tower observations, with and without energy closure adjustment, are given for each site as mean monthly diurnal cycles of  $LE$  (Figure 3) and as the monthly  $LE$  time series (Figure 4). The period of record mean  $LE$  and  $ET$  for Thurston Ola'a are given in Table 3.

Table 3. Mean annual latent energy flux ( $W\ m^{-2}$ ) and evapotranspiration ( $mm\ yr^{-1}$ ).

	Thurston	Ola'a
<hr/> Latent energy flux ( $W\ m^{-2}$ )		
Unadjusted	47.04	56.76
Adjusted	57.80	61.49
<hr/> Evapotranspiration ( $mm\ yr^{-1}$ )		
Unadjusted	606	731
Adjusted	744	792
<hr/> Site Comparison (ratio)		
Ola'a/Thurston Unadjusted	1.21	
Ola'a/Thurston Adjusted	1.06	



(b)

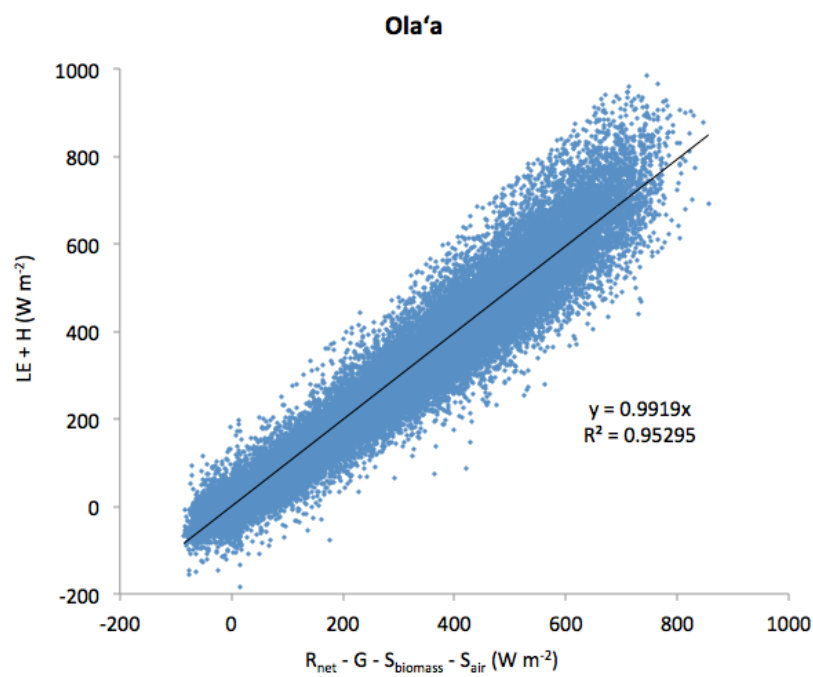


Figure 1. Energy closure for (a) Thurston and (b) Ola'a Towers.

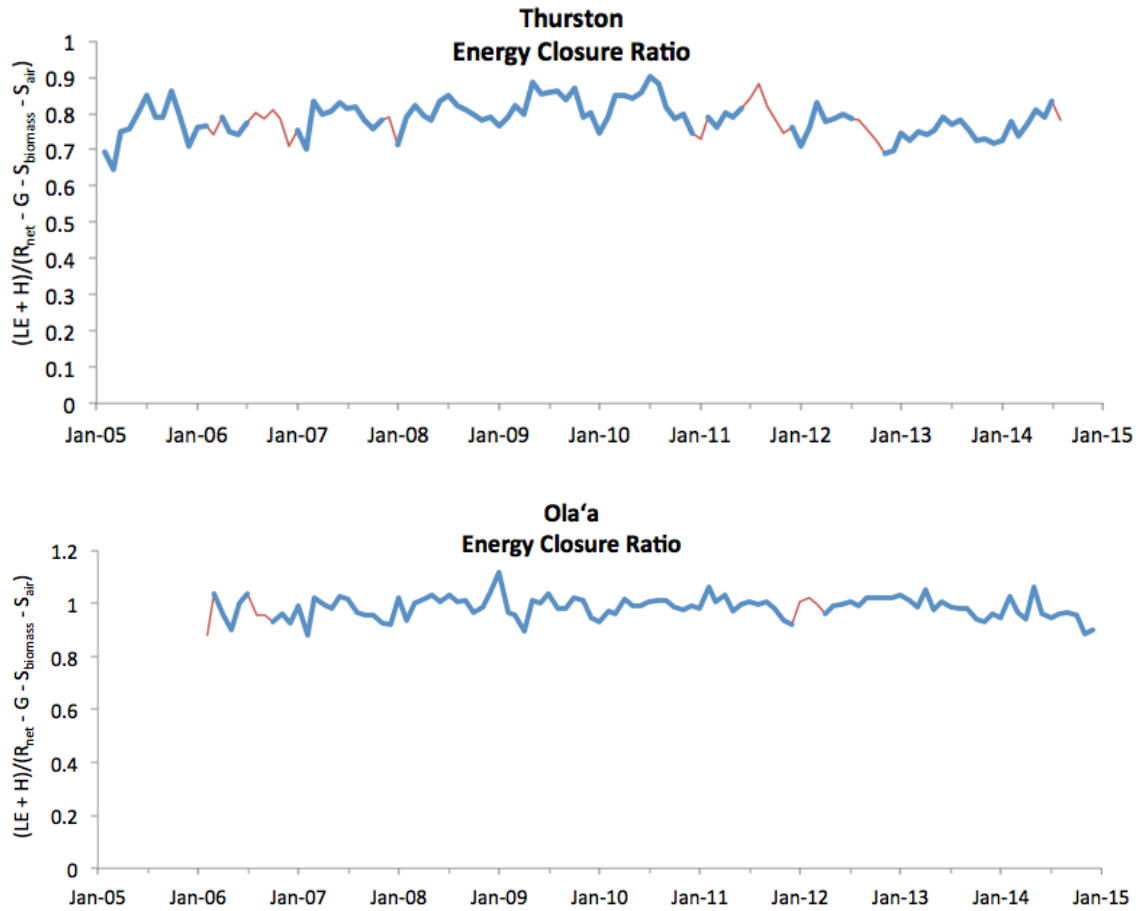


Figure 2. Time series of monthly energy closure ratio  $((LE + H)/(R_{net} - G - S_{biomass} - S_{air}))$  for (a) Thurston and (b) Ola'a . Thin red line shows values gap-filled by interpolation.

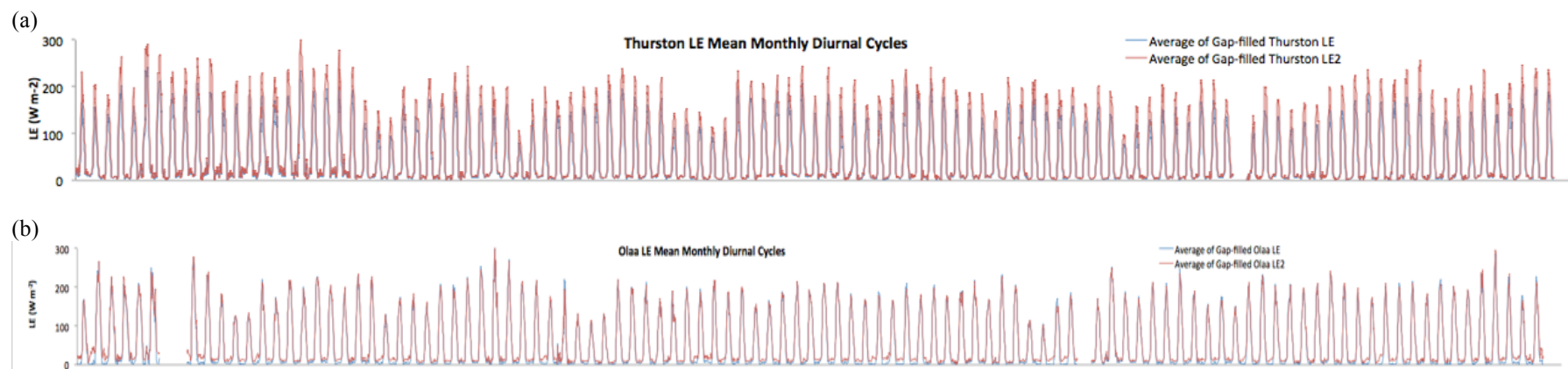


Figure 3. Mean monthly diurnal cycles of 30-min latent energy flux (LE) for (a) Thurston (native forest site) and (b) Ola'a (non-native forest site).

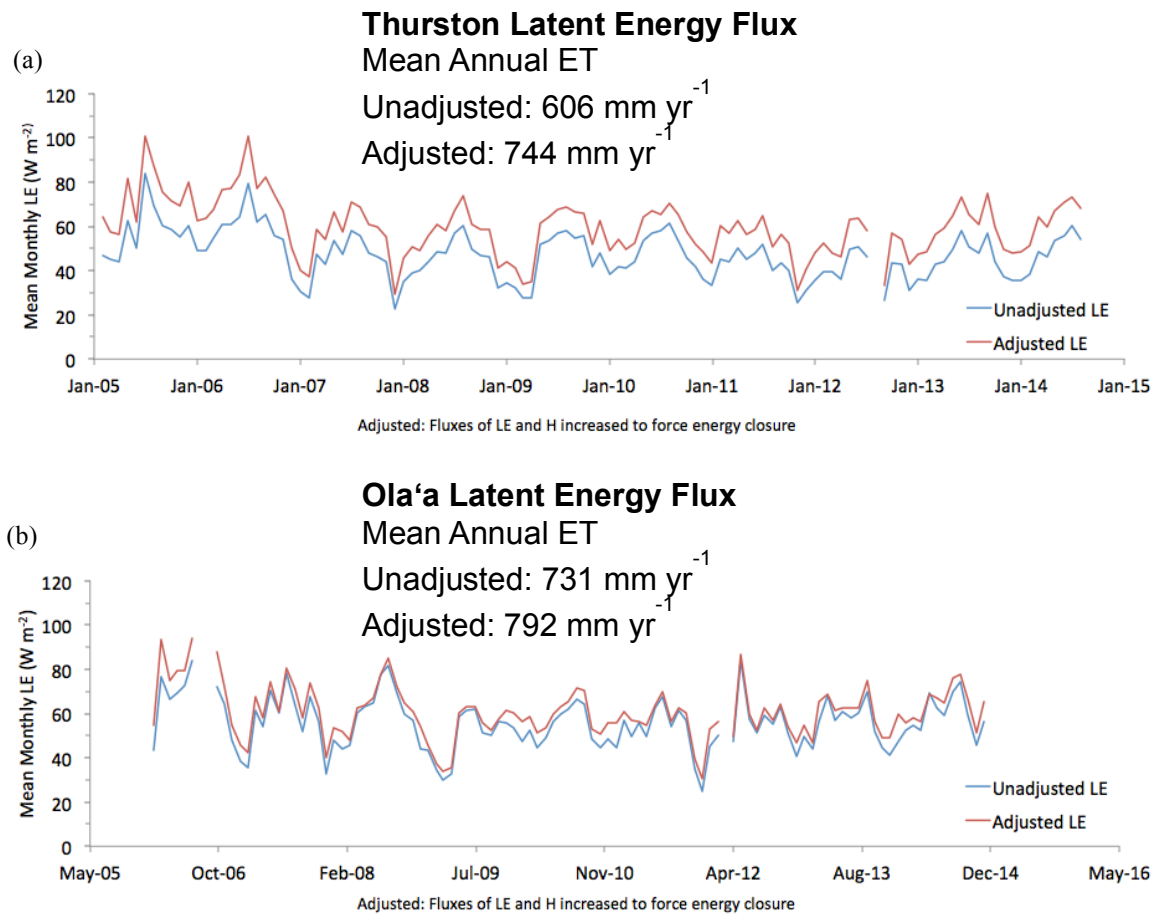


Figure 4. Mean monthly latent energy flux (LE) for (a) Thurston (native forest site) and (b) Ola'a (non-native forest site).

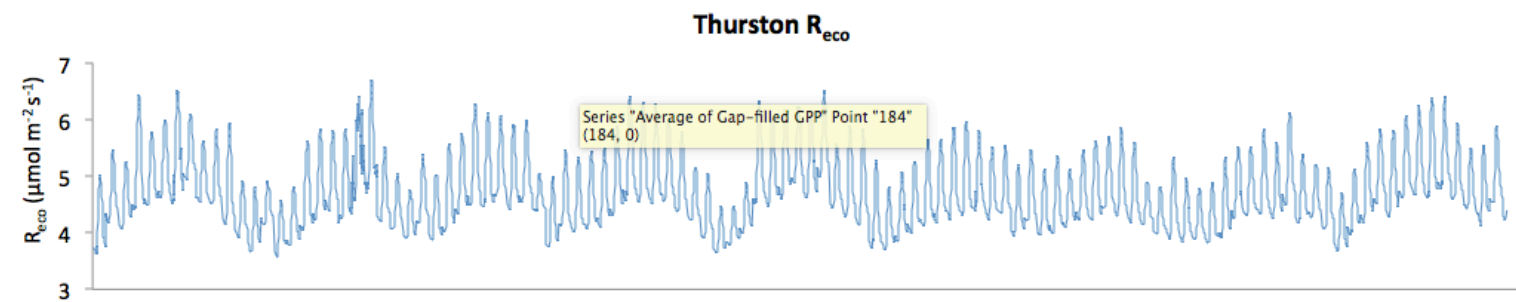
### *Carbon Flux*

The results of the carbon flux estimates derived from tower observations are given for each site as mean monthly diurnal cycles of  $R_{eco}$ , GPP, and NEE (Figures 5 and 6) and as the monthly  $R_{eco}$ , GPP, and NEE time series (Figure 7 and 8). Table 4 summarizes mean annual  $R_{eco}$ , GPP, and NEE for each site.

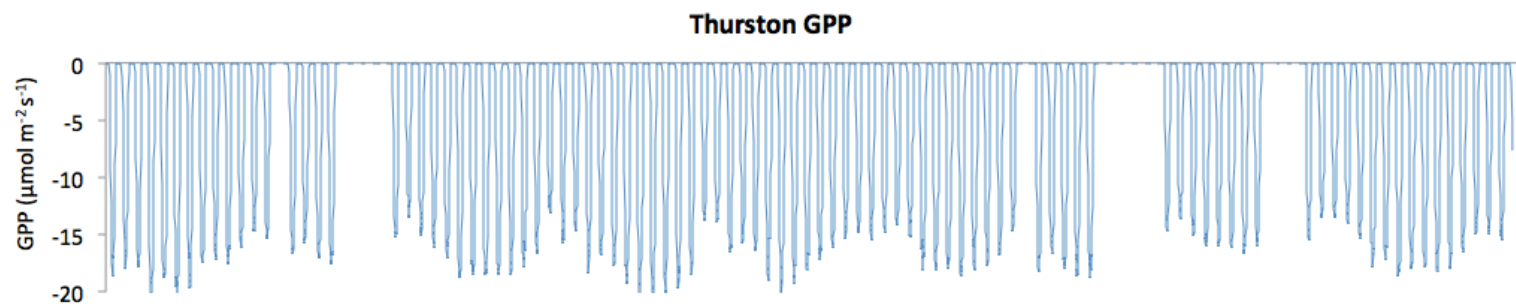
Table 4. Mean annual fluxes of carbon at the Thurston and Ola'a field sites: ecosystem respiration ( $R_{eco}$ ), gross primary production (GPP), and net ecosystem exchange (NEE).

C Fluxes ( $\mu\text{mol m}^{-2} \text{s}^{-1}$ )	<b><math>R_{eco}</math></b>	<b>GPP</b>	<b>NEE</b>
Thurston	4.751	-5.864	-1.112
Ola'a	7.018	-7.895	-0.902
C Fluxes ( $\text{Mg ha}^{-1} \text{yr}^{-1}$ )			
Thurston	18.0	22.2	4.21
Ola'a	26.6	29.9	3.42
Site comparison (ratio)			
Ola'a/Thurston	1.48	1.35	0.81

(a)



(b)



(c)

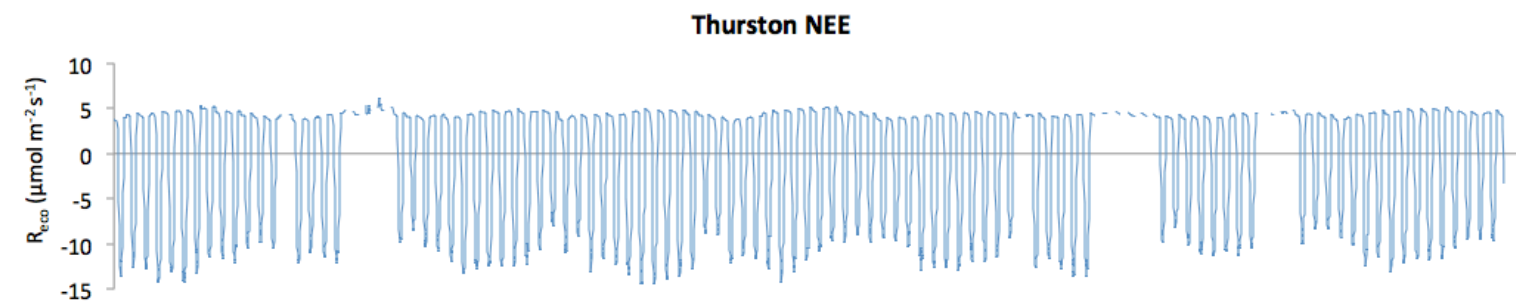
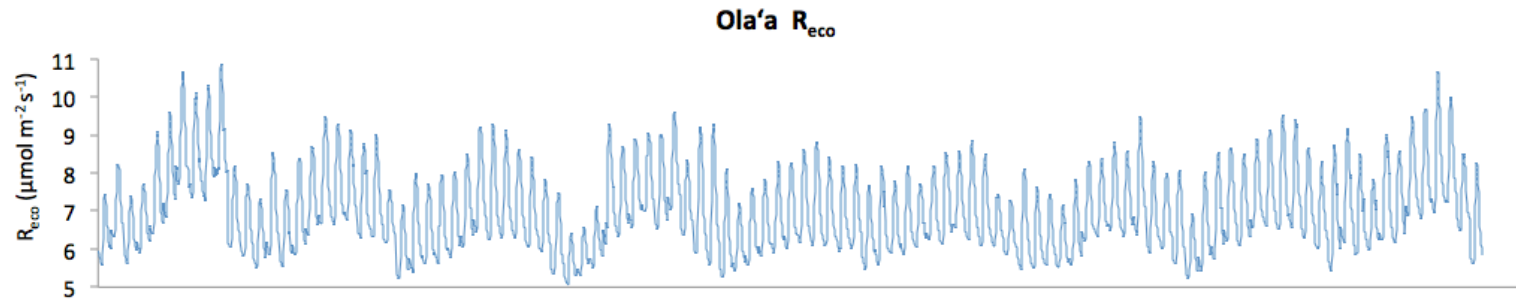
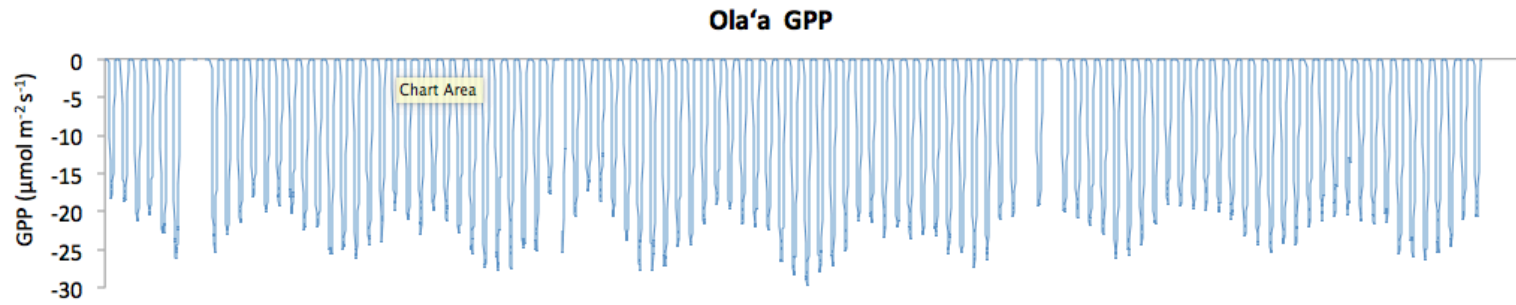


Figure 5. Monthly mean diurnal cycles of ecosystem carbon fluxes, (a) ecosystem respiration ( $R_{eco}$ ), (b) gross primary production (GPP), and (c) net ecosystem exchange (NEE) at the Thurston (native forest) study site.

(a)



(b)



(c)

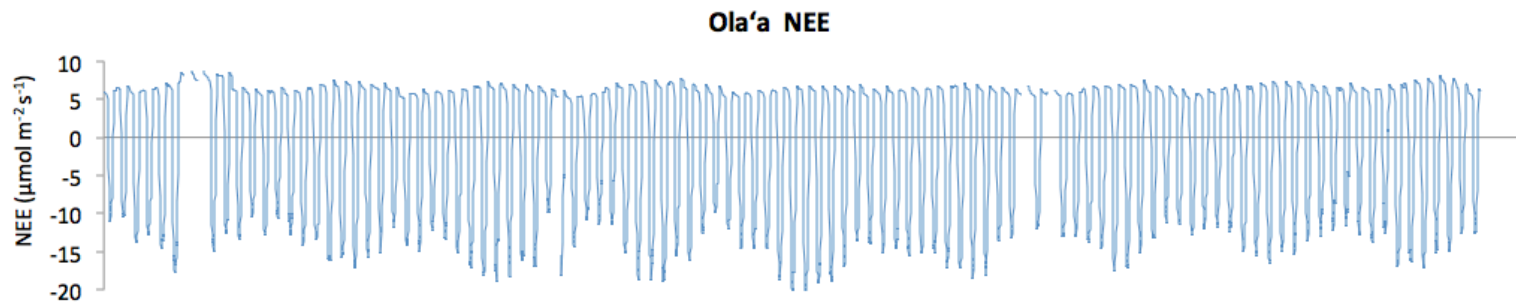


Figure 6. Monthly mean diurnal cycles of ecosystem carbon fluxes, (a) ecosystem respiration ( $R_{eco}$ ), (b) gross primary production (GPP), and (c) net ecosystem exchange (NEE) at the Ola'a (non-native forest) study site.

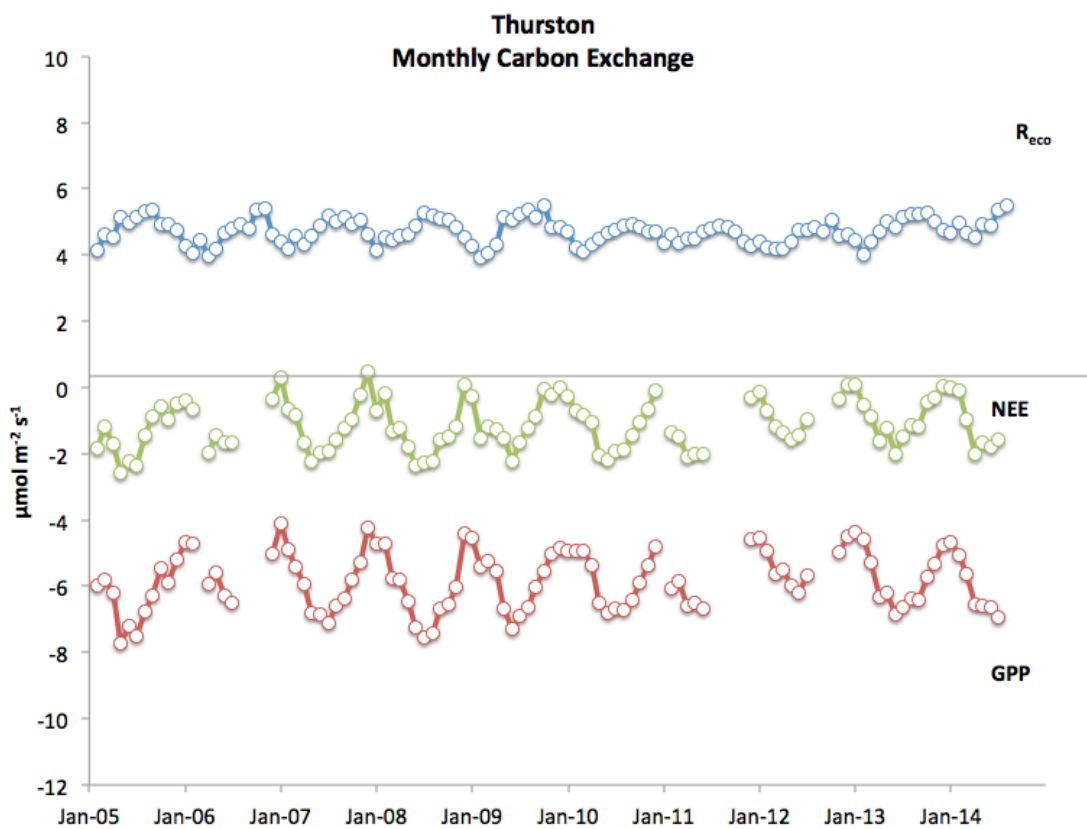


Figure 7. Mean monthly carbon fluxes: ecosystem respiration ( $R_{\text{eco}}$ ), net ecosystem exchange (NEE), and gross primary production (GPP) for Thurston (native forest site).

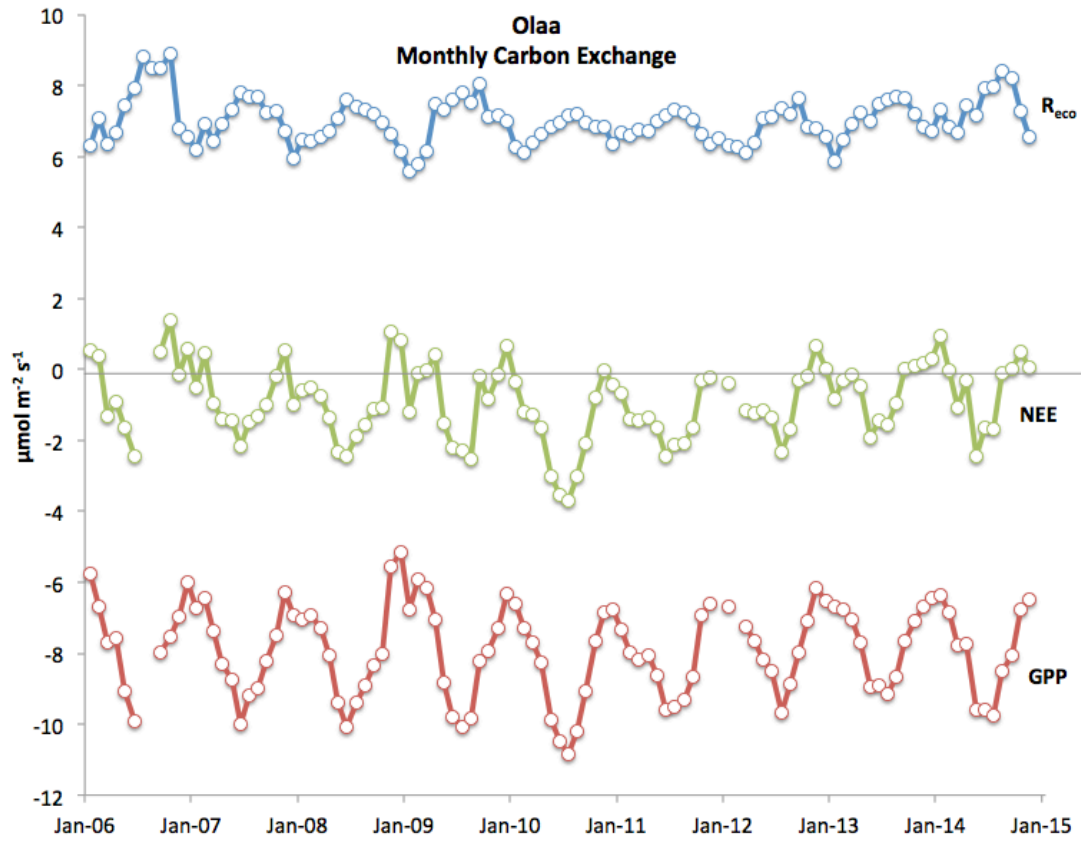


Figure 8. Mean monthly carbon fluxes: ecosystem respiration ( $R_{\text{eco}}$ ), net ecosystem exchange (NEE), and gross primary production (GPP) Ola'a (non-native forest site).

### *Sensitivity of ecosystem fluxes to climate variability*

As first order test of the sensitivity of ecosystem fluxes to climate variations, gap-filled data from each set were aggregated to a monthly interval. Aggregation was done by first including only complete rows of data for independent variable and each of the dependent variables. This process was repeated for each combination of independent and dependent variables to maximize the sample size. The 30-min-resolution mean diurnal cycle of each individual month was then calculated for each variable. Monthly means were calculated as the average of the mean diurnal cycle of the month.

Bivariate linear regression was used to assess the sensitivity of each environmental variable. See Tables 6-10.

Table 5. Environmental and flux variables tested for Thurston.

Environmental Variables	
Variable	Description
Rnet	Net radiation ( $\text{W m}^{-2}$ )
Kdn	Solar radiation ( $\text{W m}^{-2}$ )
PAR	Photosynthetically active radiation ( $\mu\text{mol m}^{-2} \text{s}^{-1}$ )
T	Air temperature ( $^{\circ}\text{C}$ )
VPD	Vapor pressure deficit (kPa)
CO2	Carbon dioxide concentration (ppm)
RF	Rainfall ( $\text{mm hr}^{-1}$ )
WS	Wind speed ( $\text{m s}^{-1}$ )
SM1	Soil moisture at 4 cm ( $\text{m}^3 \text{m}^{-3}$ )
SM2	Soil moisture at 21 cm ( $\text{m}^3 \text{m}^{-3}$ )
SM3	Soil moisture at 34 cm ( $\text{m}^3 \text{m}^{-3}$ )
FW	Canopy wetness fraction
PE-e	Energy term of potential latent energy flux ( $\text{W m}^{-2}$ )
PE-a	Aerodynamic term of potential latent energy flux ( $\text{W m}^{-2}$ )
PE	Potential latent energy flux ( $\text{W m}^{-2}$ )
Flux Variables	
Variable	Description
LE_dry	Latent energy flux with canopy conductance for dry canopy ( $\text{W m}^{-2}$ )
LE_dry_	Adjusted latent energy flux with canopy conductance for dry canopy ( $\text{W m}^{-2}$ )
LE	Latent energy flux ( $\text{W m}^{-2}$ )
LE_adj	Adjusted latent energy flux ( $\text{W m}^{-2}$ )
Reco	Ecosystem respiration ( $\mu\text{mol m}^{-2} \text{s}^{-1}$ )
GPP	Gross primary production ( $\mu\text{mol m}^{-2} \text{s}^{-1}$ )
NEE	Net ecosystem exchange ( $\mu\text{mol m}^{-2} \text{s}^{-1}$ )

Table 6. Environmental and flux variables tested for Ola'a .

Environmental Variables	
Variable	Description
Rnet	Net radiation ( $\text{W m}^{-2}$ )
Kdn	Solar radiation ( $\text{W m}^{-2}$ )
PAR	Photosynthetically active radiation ( $\mu\text{mol m}^{-2} \text{s}^{-1}$ )
T	Air temperature ( $^{\circ}\text{C}$ )
VPD	Vapor pressure deficit (kPa)
CO2	Carbon dioxide concentration (ppm)
RF	Rainfall ( $\text{mm hr}^{-1}$ )
WS	Wind speed ( $\text{m s}^{-1}$ )
SM1	Soil moisture at 4 cm ( $\text{m}^3 \text{m}^{-3}$ )
SM2	Soil moisture at 0-30 cm ( $\text{m}^3 \text{m}^{-3}$ )
SM3	Soil moisture at 28-58 cm ( $\text{m}^3 \text{m}^{-3}$ )
SM4	Soil moisture at 183-213 cm ( $\text{m}^3 \text{m}^{-3}$ )
SM5	Soil moisture at 58-88 cm ( $\text{m}^3 \text{m}^{-3}$ )
SM6	Soil moisture at 88-119 cm ( $\text{m}^3 \text{m}^{-3}$ )
SM7	Soil moisture at 118-149 cm ( $\text{m}^3 \text{m}^{-3}$ )
FW	Canopy wetness fraction (ratio)
PE-e	Energy term of potential latent energy flux ( $\text{W m}^{-2}$ )
PE-a	Aerodynamic term of potential latent energy flux ( $\text{W m}^{-2}$ )
PE	Potential latent energy flux ( $\text{W m}^{-2}$ )
Flux Variables	
Variable	Description
LE_dry	Latent energy flux with canopy conductance for dry canopy ( $\text{W m}^{-2}$ )
LE_dry_	Adjusted latent energy flux with canopy cond. for dry canopy ( $\text{W m}^{-2}$ )
LE	Latent energy flux ( $\text{W m}^{-2}$ )
LE_adj	Adjusted latent energy flux ( $\text{W m}^{-2}$ )
Reco	Ecosystem respiration ( $\mu\text{mol m}^{-2} \text{s}^{-1}$ )
GPP	Gross primary production ( $\mu\text{mol m}^{-2} \text{s}^{-1}$ )
NEE	Net ecosystem exchange ( $\mu\text{mol m}^{-2} \text{s}^{-1}$ )

Table 7. Variance in latent energy flux (evapotranspiration) explained by variance in environmental variables ( $r^2$ ) at Thurston; based on gap-filled monthly time series.

Variable	Sign	LE_dry	LE_dry_adj	LE	LE-adj
Rnet	+	0.669	0.559	0.416	0.385
Kdn	+	0.799	0.713	0.610	0.584
PAR	+	0.810	0.728	0.657	0.627
T	+	0.332	0.298	0.192	0.196
VPD	+	0.374	0.468	0.515	0.581
CO2	0	0.003	0.007	0.026	0.011
RF	-	0.199	0.227	0.259	0.275
WS	+	0.062	0.028	0.055	0.031
SM1	-	0.059	0.056	0.025	0.031
SM2	-	0.313	0.321	0.262	0.280
SM3	-	0.108	0.106	0.088	0.090
FW	-	0.296	0.295	0.171	0.195
PE-e	+	0.729	0.616	0.461	0.431
PE-a	+	0.565	0.667	0.637	0.716
PE	+	0.909	0.891	0.751	0.770

Table 8. Variance in latent energy flux (evapotranspiration) explained by variance in environmental variables ( $r^2$ ) at Ola'a; based on gap-filled monthly time series.

	Sign	LE_dry	LE-dry_adj	LE	LE-adj
Rnet	+	0.524	0.366	0.267	0.223
Kdn	+	0.680	0.532	0.455	0.406
PAR	+	0.680	0.532	0.455	0.406
T	+	0.297	0.258	0.182	0.179
VPD	+	0.543	0.660	0.706	0.754
CO2	0	0.000	0.003	0.001	0.000
RF	-	0.204	0.200	0.219	0.214
WS	+	0.021	0.001	0.009	0.002
SM1	-	0.214	0.191	0.226	0.198
SM2	-	0.049	0.085	0.044	0.071
SM3	-	0.213	0.225	0.220	0.224
SM4	-	0.049	0.066	0.069	0.076
SM5	-	0.306	0.321	0.309	0.313
SM6	-	0.245	0.262	0.274	0.279
SM7	-	0.186	0.200	0.226	0.227
FW	-	0.061	0.036	0.000	0.000
PE-e	+	0.583	0.420	0.312	0.267
PE-a	+	0.529	0.664	0.739	0.801
PE	+	0.886	0.877	0.840	0.840

Table 9. Statistical results of sensitivity tests of ecosystem carbon fluxes in response to fluctuations in environmental variables at Thurston.

	$R_{eco} (+)^*$		GPP (-)		NEE (-)	
	$r^2$	Slope	$r^2$	Slope	$r^2$	Slope
PAR	0.16	0.0021	0.71	-0.0100	0.64	-0.0082
T	1.00	0.3239	0.32	-0.4240	0.03	-0.1000
VDP	0.17	4.1830	0.05	-5.1510	0.00	-0.9680
CO2	0.00	-0.0015	0.03	0.0150	0.03	0.0130
RF	0.07	-0.9420	0.16	3.3770	0.12	2.4340
WS	0.22	-0.4230	0.14	-0.4010	0.22	-0.4230
SM4	0.01	-0.9100	0.05	4.3560	0.05	3.4470
SM21	0.13	-8.0600	0.07	11.7280	0.07	11.7280
SM34	0.05	-2.5650	0.05	6.7410	0.03	4.1770
FW	0.11	-1.8960	0.20	6.0670	0.14	4.1710

\*Sign convention is positive for flux from the ecosystem to the atmosphere. Hence,  $R_{eco}$  is inherently positive (+), and GPP, expressed under this convention is negative (-). NEE is negative (-) for ecosystems acting as a carbon sink, as is the case for the Thurston site.

Table 10. Statistical results of sensitivity tests of ecosystem carbon fluxes in response to fluctuations in environmental variables at Ola'a .

	$R_{eco} (+)^*$		GPP (-)		NEE (-)	
	$r^2$	Slope	$r^2$	$r^2$	Slope	$r^2$
PAR	0.16	0.0039	0.63	-0.0167	0.53	-0.01279
T	0.99	0.5249	0.34	-0.6457	0.02	-0.12077
VPD	0.24	6.8577	0.01	-3.0600	0.02	3.79768
CO2	0.00	-0.0036	0.12	0.0465	0.13	0.04294
RF	0.02	-0.0074	0.08	0.0328	0.07	0.02542
WS	0.04	-0.9336	0.09	2.9004	0.06	1.96682
SM1	0.10	-3.8019	0.05	5.8810	0.01	2.07912
SM2	0.08	-4.0534	0.01	3.4680	0.00	-0.58535
SM3	0.18	-20.6551	0.09	31.0902	0.01	10.43512
SM4	0.06	-29.5009	0.02	32.9680	0.00	3.46705
SM5	0.35	-25.9269	0.17	40.3630	0.03	14.43606
SM6	0.26	-29.2242	0.11	40.9805	0.01	11.75625
SM7	0.20	-24.4584	0.09	33.8664	0.01	9.40806
FW	0.16	-3.3832	0.23	8.5355	0.12	5.15230

\*Sign convention is positive for flux from the ecosystem to the atmosphere. Hence,  $R_{eco}$  is inherently positive (+), and GPP, expressed under this convention is negative (-). NEE is negative (-) for ecosystems acting as a carbon sink, as is the case for the Ola'a site.

### *Evapotranspiration Sensitivity to Variations in Environmental Conditions*

Using multiple regression analysis and after testing of alternative predictor variable combinations, the best statistical models of LE<sub>adj</sub> are:

$$\text{Thurston: LE}_{\text{adj}} = -42.70 + 0.207 * \text{RNET} + 242.58 * \text{VPD} + 67.431 * \text{FW} \quad (4)$$

Multiple R-squared: 0.867

Residual standard error: 4.322

$$\text{Ola'a: LE}_{\text{adj}} = -24.73 + 0.256 * \text{RNET} + 138.92 * \text{VPD} + 42.957 * \text{FW} \quad (5)$$

Multiple R-squared: 0.859

Residual standard error: 5.152

### *Carbon Flux Sensitivity to Variations in Environmental Conditions*

Using multiple regression analysis and after testing of alternative predictor variable combinations, the best statistical models of NEE are:

$$\text{Thurston: NEE} = 1.770 - 0.00855 * \text{PAR} + 2.2440 * \text{VPD} \quad (6)$$

Multiple R-squared: 0.705

Residual standard error: 0.451

$$\text{Ola'a: NEE} = 2.178 - 0.01553 * \text{PAR} + 10.0357 * \text{VPD} \quad (7)$$

Multiple R-squared: 0.716

Residual standard error: 0.641

### *Projected Effects of Climate Change on Ecosystem Fluxes*

The statistical models of ecosystem fluxes given above identify R<sub>net</sub>, VPD, FW, and PAR as predictors. The downscaled climate projections used to set the climate scenarios for this project do not directly provide estimates of changes in these variables. As a simple method of estimating plausible changes consistent with projected changes in T and rainfall, linear regression of monthly data at the study sites was used. On that basis, a T change of +3.5°C implies a VPD change of +0.0392 kPa. The projected rainfall changes of 0 -30, -20, and -50%, imply PAR changes of 0, +2.9, +1.9, and +4.8%, respectively. R<sub>net</sub> is highly correlated with PAR, and was estimated as a function of PAR with site-specific linear regression equations. Applying those changes to the multiple regression model yields changes in evapotranspiration (adjusted LE) and NEE shown in Tables 11 and 12.

Table 11. Projected change in evapotranspiration (LE<sub>adj</sub>; %) as a result of estimated changes in R<sub>net</sub> and VPD based on multiple regression models at each site.

	LE <sub>adj</sub> Change from Present			
	Thurston		Ola'a	
	Wet Season	Dry Season	Wet Season	Dry Season
Scenario 1	+10.1%	+12.5%	+19.0%	+18.4%
Scenario 2	+11.7%	+14.1%	+20.1%	+14.5%

Table 12. Projected change in net ecosystem carbon exchange (NEE; %) as a result of estimated changes in PAR and VPD based on multiple regression models at each site.

	NEE Change from Present			
	Thurston		Ola'a	
	Wet Season	Dry Season	Wet Season	Dry Season
Scenario 1	-8.9%	-0.6%	-24.3%	-14.2%
Scenario 2	-3.3%	+5.0%	-17.1%	-7.5%

## ANALYSIS AND FINDINGS:

### *Flux Differences Between the Study Sites*

Mean annual LE for the two sites was 47 and 57  $\text{W m}^{-2}$ , respectively, for Thurston and Ola'a. After adjustment for energy closure, mean annual estimates for the two sites were much more similar to each other at 58 and 61  $\text{W m}^{-2}$ , respectively. In either case, LE (ET), was higher at Ola'a than Thurston, despite lower  $R_{\text{net}}$  and more humid conditions at Ola'a. Normalizing by  $R_{\text{net}}$ , allows us to control for the difference in available energy at the two sites.  $\text{LE}/R_{\text{net}}$  was 47% higher at Ola'a than Thurston (unadjusted) and 43% higher after energy closure adjustment. This difference suggests that given the same radiative input, ET at the non-native site (Ola'a) would be much higher than at the native site (Thurston).

Mean annual ecosystem respiration ( $R_{\text{eco}}$ ) was 48% higher at Ola'a than Thurston. Likewise, GPP was 35% higher at Ola'a. As a result, NEE was 19% lower at Ola'a than Thurston. Thus, despite much higher photosynthesis at Ola'a, the overall growth of the system is lower according to the tower measurements. Hence, carbon cycling is much more rapid at the non-native site, while overall carbon accumulation is slower. Higher respiration at Ola'a is consistent with higher temperature at this site (because of its slightly lower elevation). But the magnitude of the difference cannot be explained by temperature alone. Differences in leaf turnover rates and decomposition are likely to be influenced by the difference in species composition. It should be noted that biometric measurements also find higher  $R_{\text{eco}}$  and GPP at Ola'a than Thurston. But, those measurements indicate that NEE is higher at Ola'a.

### *Sensitivity of Fluxes to Variations in Environmental Conditions*

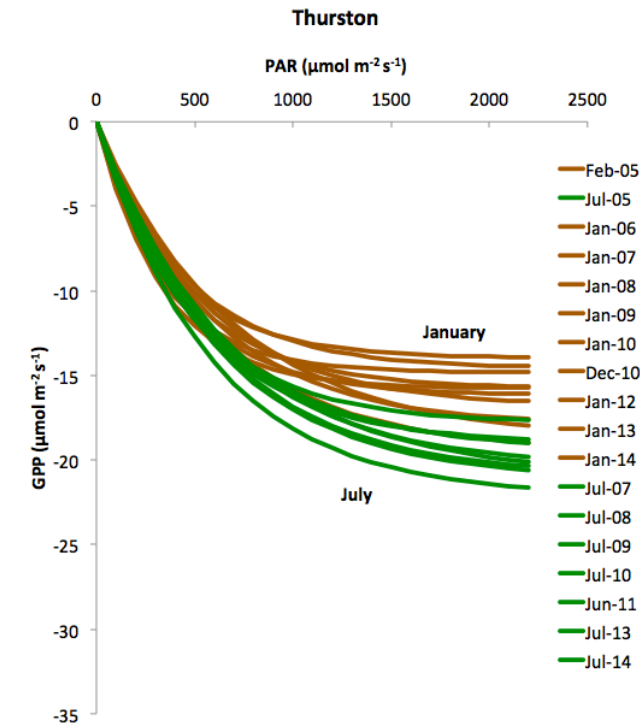
The statistical models of ecosystem flux for the two sites are similar in that they are based on the same predictor variables:  $R_{\text{net}}$ , VPD, and FW for evapotranspiration  $\text{LE}_{\text{adj}}$ , and PAR and VPD for net carbon uptake (NEE). However, the sites differ in their sensitivities to environmental conditions in several ways. GPP is much more responsive to PAR variations at Ola'a than at Thurston, especially during the summer.  $R_{\text{eco}}$  is also more responsive to T at Ola'a. NEE sensitivity to both PAR and T is significantly greater at Ola'a.

The finding that ET is slightly higher at Ola'a than Thurston, but much higher at Ola'a when normalized by  $R_{\text{net}}$  is consistent with previous findings for the site (Giambelluca et al. 2009). Takahashi et al. (2011) found that wet canopy evaporation was significantly lower at Ola'a than Thurston suggesting that transpiration at the non-native site is high compared with that of the native site.

Carbon exchanges are significantly different for the two sites. GPP is 35% greater at Ola'a than Thurston. This is explained by the much higher light response for Ola'a (Figure 9). Note that

typical summer midday values are in the 25-30  $\mu\text{mol m}^{-2} \text{s}^{-1}$  range at Ola'a and mostly less than 20  $\mu\text{mol m}^{-2} \text{s}^{-1}$  at Thurston. In addition, solar radiation is significantly higher at Thurston than Ola'a because of less frequent cloud cover.

(a)



(b)

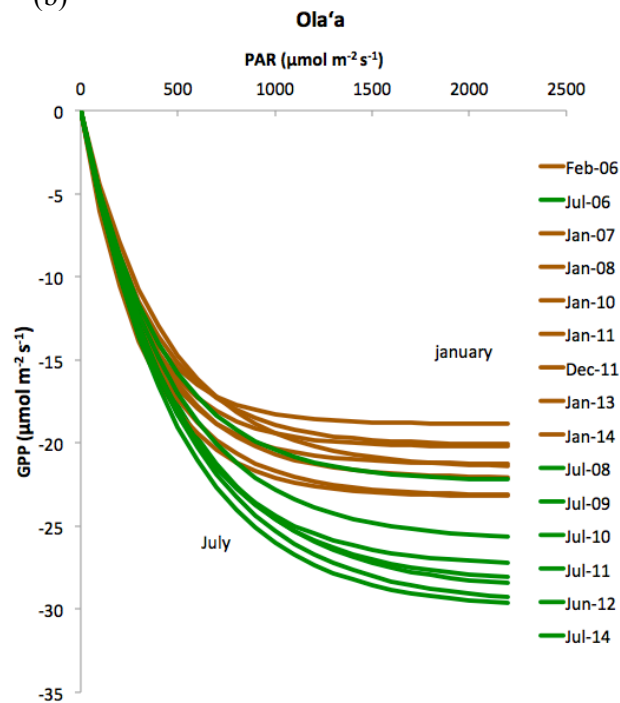


Figure 9. January and July light response curves for (a) Thurston and (b) Ola'a.

### *Flux sensitivity*

Evapotranspiration sensitivity to environmental variables is widely studied. In general, the ET rate is determined by the available energy (mainly  $R_{\text{net}}$ ), the drying power of the air (VPD and wind speed), the roughness of the surface (height and unevenness of vegetation), and moisture availability (amount of water stored in the soil and on the canopy). Statistical analysis of the flux data show that LE responds most strongly to energy input as measured by any of the radiation variables ( $R_{\text{net}}$ ,  $K_{\text{dn}}$ , or PAR), VPD, and air temperature, although the relationship with the latter two variables is partially explained by multicollinearity between them and radiation. Moisture variables all have negative relationships with LE, opposite of what would be expected in a water limited environment. Again the negative relationship with these variables can be explained by the negative relationship between them and radiation. We conclude that ET at both of these sites is controlled mainly by variations in energy. Atmospheric drying power, driven by fluctuations in temperature, humidity, and wind, has a secondary influence, especially under wet canopy conditions. The sites differ moderately in the importance of aerodynamic influences, with Ola'a more responsive to variations in VPD than Thurston. Temperature has almost identical effects on ET at the two sites.

Carbon flux sensitivity is also dominated by radiation. Evidence strongly indicates that carbon fluxes at the two sites are light limited. PAR is the mostly highly correlated variable with GPP. In part, this is an artifact of the GPP estimation technique. But, the evidence is strong that light availability is the main limiting factor.  $R_{\text{eco}}$  has a very high correlation with T, but this is a result of the temperature-based estimation method used to gap fill the data. In fact, the relationship between nighttime NEE (assumed to be equal to  $R_{\text{eco}}$ ) and temperature is weak. No relationship was found between measured nighttime NEE and soil moisture.  $R_{\text{eco}}$  values obtained in this analysis are consistent with independent estimates from biometric data (this report). GPP is positively correlated with T. This relationship is not fully explained by T – PAR multicollinearity, and it is consistent with the known influence of temperature on photosynthesis in wet forests. The two apparent influences of temperature on carbon fluxes, therefore, oppose each other. Increasing T would increase gross uptake (higher GPP), but also increase loss (higher  $R_{\text{eco}}$ ). These opposing effects offset each other, reducing the net effect of T (small sensitivity of NEE to T). VPD has a significant negative effect on NEE, consistent with typical stomatal conductance response.

These results conflict to some extent with those based on leaf-level measurements (Task 3, this report), which indicate very similar per-leaf-area gas exchange rates for the principal species at the two sites.

## CONCLUSIONS:

Preliminary conclusions derived from analysis of the flux tower observations at the two study sites:

- Evapotranspiration is controlled mainly by variations in energy at both sites.
- Evapotranspiration is slightly greater at Ola'a than Thurston.
- When controlled for available energy, evapotranspiration is significantly higher at Ola'a than Thurston.
- NEE is controlled mainly by PAR and secondarily by VPD at both sites
- GPP light response is significantly greater at Ola'a than Thurston, especially during the summer.
- At both sites, based on a simple statistical approach, projected changes in climate will cause significant increases in evapotranspiration.
- Based on these projections of increased ET, climate change will cause significant negative changes in water availability for groundwater recharge and streamflow generation.
- At Thurston, based on a simple statistical approach, projected changes in climate will cause small to moderate reductions in growth in the wet season and no change to small increase in growth in the dry season.
- At Ola'a, based on a simple statistical approach, projected changes in climate will cause large reductions in growth rates in the wet season and moderate reductions in growth rates in the dry season.
- Based on these projections of changes in NEE, climate change will cause significant reductions in growth rates at Ola'a, and smaller changes in growth rates at Thurston.

## References Cited

- Baldocchi, D. D., B. B. Hicks, T. P. Meyers (1988), Measuring biosphere-atmosphere exchanges of biologically related gases with micrometeorological methods, *Ecol.*, 69, 1331-1340.
- Elison Timm, O., and Fortini, L. (2016) Statistical estimation of future temperature anomalies. Data product. [http://www.atmos.albany.edu/facstaff/timm/products\\_data.html](http://www.atmos.albany.edu/facstaff/timm/products_data.html)
- Elison Timm, O., Giambelluca, T.W., and Diaz, H.F. 2015. Statistical downscaling of rainfall changes in Hawai'i based on the CMIP5 global model projections. *Journal of Geophysical Research-Atmospheres* 120: 92-112, doi: 10.1002/2014JD022059.
- Fisher, J. B., Y. Malhi, D. Bonal, et al. (2009), The land-atmosphere water flux in the tropics, *Global Change Biol.*, 15, 2694-2714.
- Giambelluca, T.W., Martin, R.E., Asner, G.P., Huang, M., Mudd, R.G., Nullet, M.A., DeLay, J.K., and Foote, D. 2009. Evapotranspiration and energy balance of native wet montane cloud forest in Hawai'i. *Agricultural and Forest Meteorology* 149: 230-243, doi: 10.1016/j.agrformet.2008.08.004.
- Goulden, M.L., Munger, J.W., Fan, S.-M., Daube, B.C., Wofsy, S.C. 1996. Measurements of carbon sequestration by long-term eddy covariance: methods and a critical evaluation of accuracy. *Global Change Biology* 2: 160-182.
- Högström et al. (1989)
- Högström, U., Bergström, H., and Smedman, A.-S. 1989. Turbulent fluxes above a pine forest, I: Fluxes and gradients. *Boundary-Layer Meteorology* 49: 197-217.

- Miller, S.D., Goulden, M.L., Menton, M.C., da Rocha, H.R., de Freitas, H.C., e Silva Figuera, A.M. 2004. Biometric and micrometeorological measurements of tropical forest carbon balance. *Ecological Applications* 14: S114-S126.
- Mudd, R.G. 2012. Heat storage and energy closure in two tropical montane forests in Hawai'i. Masters' thesis, Geography, University of Hawai'i at Mānoa, Honolulu, USA.
- Noormets, A., Chen, J., and Crow, T. R.. 2007. Age-dependent changes in ecosystem carbon fluxes in managed forests in northern Wisconsin, USA. *Ecosystems* 10: 187-203.
- Saleska et al. 2003. Carbon in Amazon forests: unexpected seasonal fluxes and disturbance-induced losses. *Science* 302: 1554-1557.
- Takahashi, M., Giambelluca, T.W., Mudd, R.G., DeLay, J.K., Nullet, M.A., and Asner, G.P. 2011. Rainfall partitioning and cloud water interception in native forest and invaded forest in Hawai'i Volcanoes National Park. *Hydrological Processes* 25: 448-464, doi: 10.1002/hyp.7797.
- Tanner, C. B. and Thurtell, G. W. 1969. *Anemoclinometer Measurements of Reynolds Stress and Heat Transport in the Atmospheric Surface Layer*. University of Wisconsin Tech. Rep., ECOM-66-G22-F, 82 pp.
- Twine, T.E., Kustas, W.P., Norman, J.M., Cook, D.R., Houser, P.R., Meyers, T.P., Prueger, J.H., Starkds, P.J., Wesely, M.L. 2000. Correcting eddy-covariance flux underestimates over a grassland. *Agricultural and Forest Meteorology* 103: 279-300.
- Webb, E.K., Pearman, G.I., and Leuning, R. 1980. Correction of flux measurements for density effects due to heat and water vapor transfer. *Quarterly Journal of the Royal Meteorological Society* 106: 67-90.
- Wilczak, J.M., Oncley, S.P., and Stage, S.A. 2001. Sonic anemometer tilt correction algorithms. *Boundary-Layer Meteorology* 99: 127-150.
- Zhang, C. X., Wang, Y., Lauer, A., and Hamilton, K. 2012. Configuration and evaluation of the WRF model for the study of Hawaiian regional climate. *Monthly Weather Review* 140: 3259-3277, doi: 10.1175/MWR-D-11-00260.1.

## Task 2: Validation of Flux Tower Observations with Biometric Measurements

### PURPOSE AND OBJECTIVES:

Differences in carbon, water, and energy fluxes between the native (Thurston) and invaded (Ola'a) sites were identified primarily via tower-based eddy covariance measurements. Biometric measurements (i.e., direct “on-the-ground” measurements of biological processes), in turn, are critical for validating and corroborating data from flux towers (Luyssaert et al. 2009). Complete carbon budgets are difficult and time-consuming to build in forest ecosystems and, as such, very few exist globally (Litton et al. 2007). Biometric measurements, however, allow for direct observation of critical components of ecosystem metabolism, albeit at lower temporal frequency and continuity than eddy covariance techniques (Luyssaert et al. 2009). For this study, we focused on four biometric measurements of ecosystem processes that are of critical importance to stand-level carbon cycling to compare with flux tower data on carbon dynamics: (i) aboveground litterfall; (ii) soil-surface CO<sub>2</sub> efflux (‘soil respiration’); (iii) aboveground biomass increment; and (iv) leaf area index (LAI). Litterfall is an easily and commonly measured carbon flux in forests that is very well correlated with stand-level productivity, and can be used to indirectly estimate stand-level gross primary production (GPP) (Litton et al. 2007). Soil-surface CO<sub>2</sub> efflux (i.e., the sum of all CO<sub>2</sub> produced belowground, including root and heterotrophic respiration, that then diffuses to the overlying atmosphere) is an excellent index of overall belowground carbon cycling (Giardina and Ryan 2002; Litton et al. 2004), and is tightly coupled with stand-level productivity (Högberg et al. 2001). In addition, soil-surface CO<sub>2</sub> efflux is the dominant component of ecosystem respiration in temperate forest ecosystems at ~70% (Janssens et al. 2001; Xu et al. 2001; Ryan and Law 2005), and can therefore be used to indirectly validate total ecosystem respiration from flux towers. Aboveground biomass increment, in turn, is the major component of aboveground net primary production and, therefore, is strongly correlated with stand-level GPP. Finally, LAI is an estimate of the quantity of photosynthetically active tissue in a forest and, as such, is an excellent index of overall stand productivity (i.e., GPP).

### ORGANIZATION AND APPROACH:

Aboveground fine litterfall consists of leaves, reproductive material, and wood <2.0 cm diameter. Annual litterfall was estimated by collecting, drying and sorting all litter at each site on a monthly basis from twenty 0.25 m<sup>2</sup> littertraps/site from September 2014 to September 2015. Stand-level GPP was then estimated from annual aboveground fine litterfall at each site by: (i) assuming that 50% of all litterfall biomass was C; and (ii) applying a global relationship between foliage production and GPP for forest ecosystems from Litton et al. (2007).

Soil-surface CO<sub>2</sub> efflux was measured at each site in May of 2014 and 2015 on sixteen 20 cm diameter PVC collars inserted 5 cm into the soil surface with an LI-8100A (LI-COR, Lincoln, NE). We then used instantaneous measurements of soil-surface CO<sub>2</sub> efflux taken at mean annual temperature (i.e., in July in our study systems) to provide a well constrained estimate of annual soil-surface CO<sub>2</sub> (Bahn et al. 2010). The utility of using instantaneous measurements of soil-surface CO<sub>2</sub> efflux at mean annual temperature to estimate annual cumulative flux of CO<sub>2</sub> from soils has been previously validated in Hawaiian tropical montane wet forests (Litton et al. 2011). Finally, we estimated the proportion of total ecosystem respiration accounted for by soil-surface CO<sub>2</sub> using our annual soil CO<sub>2</sub> flux estimates from biometric measurements and total ecosystem respiration estimates from the flux towers.

Aboveground live biomass carbon density (AGCD) and increment growth was measured as the difference between two long-term plot-level survey measurements in four 10x10 m plots at the

native site and six 10x10 m plots at the invaded site. Initial measurements were conducted in 2004 and 2006, with final measurements conducted in 2016. Therefore, AGCD was estimated for approximately the same period as carbon flux measurements from the tower reported herein. Measurements of all individual trees >5 cm DBH and all tree ferns were scaled to AGCD using species specific allometric relationships between diameter at 1.3 m ( $D_{BH}$ , cm) and dry biomass obtained from the literature, with carbon assumed to be half of dry biomass. Because smaller individuals of *P. cattleianum* represent an unusually large proportion of biomass at the invaded site, individuals between 2-5 cm were measured in two of the six plots and scaled to the stand. Total aboveground dry stem and leaf biomass for *M. polymorpha* and *P. cattleianum* was calculated from species specific allometric equations (Mascaro et al., 2011; model 1) relating  $D_{BH}$  to plant dry biomass. To determine the biomass of tree ferns (*Cibotium* spp.), stem volume of all individuals were determined from survey data, and an allometric model (Arcand et al. 2008) was used to estimate dry leaf mass based on frond radius at the native site. Frond radius of tree ferns was not measured in the survey at the invaded site, so caudex height was used as a predictor for frond biomass prediction there. Allometric models for *I. anomala* and *C. trigynum* (Raich et al. 1997) do not include any individuals greater than 10 cm  $D_{BH}$ , and thus cannot be reasonably extrapolated to the larger size range of trees at the study sites. For these tree species, the *M. polymorpha* model was used, and to correct for differential wood density modeled biomass was multiplied by the ratio of *I. anomala* and *C. trigynum* wood density to *M. polymorpha* wood density (Asner et al. 2011).

Leaf area index was measured indirectly at each site (May 2014 at the native site and June 2015 at the invaded site) using an LAI-2200 (LI-COR, Lincoln, NE) by taking below- and above-canopy measurements of simultaneously and inferring leaf area from measurements of how radiation is intercepted by the canopy using a simple light interception model. Below canopy observations ( $n=20$ ) were taken at 5 m intervals along a 100 m transect intersecting the littertraps within each site. Above canopy observations were taken from the meteorological tower, immediately downwind from the transect.

## PROJECT RESULTS:

Aboveground fine litterfall was 60.4% higher at the invaded than the native site (Table 1). At the invaded site, the non-native tree *P. cattleianum* accounted for 17.6% of total litterfall (Table 1). Stand level GPP estimated from litterfall showed values of  $1,121.9 \text{ g C m}^{-2} \text{ yr}^{-1}$  for the native site, and  $1,800 \text{ g C m}^{-2} \text{ yr}^{-1}$  for the invaded site, and once again the nonnative tree accounted for 17.6% of stand productivity at the invaded site (Table 1). Discounting production associated with the nonnative tree, stand level litterfall and GPP associated with native species was 32.3% higher at the invaded site (Table 1).

Table 1. Aboveground fine litterfall and gross primary production for the native (Thurston) and invaded (Ola'a) sites.

Site	Aboveground Litterfall (g biomass m <sup>-2</sup> yr <sup>-1</sup> )	Aboveground Litterfall (g C m <sup>-2</sup> yr <sup>-1</sup> )	GPP (g C m <sup>-2</sup> yr <sup>-1</sup> )
Thurston Total	179.50	89.8	1121.9
Ola'a Total	288.00	144.0	1800.0
Ola'a Native	237.40	118.7	1483.8
Ola'a Guava	50.60	25.3	316.3

Soil-surface CO<sub>2</sub> efflux was 38.2 and 81.8% higher at the invaded than the native site in 2014 and 2015, respectively (Table 2). These values agree well with previously published values for similar forests under similar conditions (Litton et al. 2011). In addition, the soil-surface CO<sub>2</sub> efflux values are in line with site differences in aboveground litterfall (see above). As a fraction of total ecosystem respiration, annual soil-surface CO<sub>2</sub> efflux accounted for 53.4 and 48.6% of ecosystem respiration (Table 2), which is lower than the 70% reported previously for temperate forests.

Table 2. Soil-surface CO<sub>2</sub> efflux (SR) measured at mean annual temperature (SR<sub>MAT</sub>), extrapolated to annual values (SR<sub>Annual</sub>), total ecosystem respiration (R<sub>Ecosystem</sub>) from tower measurements for 2014, and the percentage of R<sub>Ecosystem</sub> accounted for by SR<sub>Annual</sub> for the native (Thurston) and invaded (Ola'a) sites.

Site	Year	SR <sub>MAT</sub>	SR <sub>Annual</sub>	R <sub>Ecosystem</sub>	R <sub>Ecosystem</sub> as SR
		(μmol CO <sub>2</sub> m <sup>-2</sup> s <sup>-1</sup> )	(g C m <sup>-2</sup> yr <sup>-1</sup> )	(g C m <sup>-2</sup> yr <sup>-1</sup> )	%
Thurston	2014	2.39	979.0	1834.3	53.4
Thurston	2015	2.24	921.0	-	-
Ola'a	2014	3.40	1353.1	2786.3	48.6
Ola'a	2015	4.27	1674.2	-	-

At the beginning of the study period, AGCD was 43% higher at the native site than the invaded site (Table 3). However, by the end of the study period AGCD of the native stand was only 16% higher than the invaded stand due to the higher growth rates at the invaded site. The invaded stand was found to accumulate carbon at a rate of 359 g C m<sup>-2</sup> yr<sup>-1</sup>, while the native stand accumulated carbon at a rate of 155 g C m<sup>-2</sup> yr<sup>-1</sup>. These results are in agreement with higher GPP and NEE at the invaded site, and are within the range of values reported by Malhi et al. (2004) for coarse wood production in neotropical forest sites (150-550 g C m<sup>-2</sup> yr<sup>-1</sup>). At the invaded site, *P. cattleianum* had considerable spatial variability between study plots (see Table X.3; a, b), and despite a very slow growth rate of individual stems (average D<sub>BH</sub> increment less than 0.1 cm yr<sup>-1</sup>), the large number of stems allowed the invasive species to contribute 41% to total AGCB on average, while native trees contributed 38%, and tree ferns contributed the remaining 21%. While native trees at the native site gained a similar amount of carbon during the study period, native trees at the invaded site grew significantly faster than at the native site.

LAI was 4.31 (S.D. = 0.49) at the native site and 5.54 (S.D. = 0.49) at the invaded site. This indirect method of estimating leaf area shows that the invaded site had 29% more leaf area available for photosynthesis and, therefore, should be expected to have higher rates of both GPP and autotrophic respiration.

Table 3. Above-ground carbon density (AGCD) and increment growth at Native and invaded sites.

		July, 2004 (Mg C ha <sup>-1</sup> )	May, 2016 (Mg C ha <sup>-1</sup> )	Growth (g C m <sup>-2</sup> yr <sup>-1</sup> )
Native Site	Species			
	Native trees	152.0	167.7	134
	<i>M. polymorpha</i>	142.5	157.2	126
	<i>Cibotium</i> spp.	8.4	10.9	21
	Total	160.4	178.5	155
Native trees include <i>M. polymorpha</i> , <i>Ilex anomala</i> , and <i>Coprosma</i> sp. Based on 4 10 x 10 m tagged plots measured over a ~12 year period. Individuals > 5 cm diameter and all tree ferns ( <i>Cibotium</i> spp. and <i>Sadleria</i> sp.)				
Invaded Site	(a) Species	July, 2006 (Mg C ha <sup>-1</sup> )	May, 2016 (Mg C ha <sup>-1</sup> )	Growth (g C m <sup>-2</sup> yr <sup>-1</sup> )
	Native trees	41.9	57.8	162
	<i>M. polymorpha</i>	35.2	49.6	147
	<i>P. cattleianum</i>	46.3	58.4	123
	<i>Cibotium</i> spp.	23.3	29.5	63
	Total	111.4	145.7	349
	Based on 4 10x10 m tagged plots re-measured after a ~10 year period			
	(b) Species	July, 2004 (Mg C ha <sup>-1</sup> )	May, 2016 (Mg C ha <sup>-1</sup> )	Growth (g C m <sup>-2</sup> yr <sup>-1</sup> )
	Native trees	49.0	59.5	89
	<i>M. polymorpha</i>	11.3	22.3	93
	<i>P. cattleianum</i>	51.7	74.8	195
	<i>Cibotium</i> spp.	25.9	37.4	97
	Total	126.6	171.7	381
Based on 2 10x10 m tagged plots re-measured after a ~12 year period For (a) and (b), native trees include <i>M. polymorpha</i> , <i>I. anomala</i> , and <i>C. trigynum</i> Individuals > 5 cm diameter, <i>P. cattleianum</i> > 2 cm diameter, and all tree ferns ( <i>Cibotium</i> spp.)				

## ANALYSIS AND FINDINGS:

Independent validation of tower-based flux results is a critical step that should be taken before reporting flux tower results (Luyssaert et al. 2009). Overall, the biometric variables measured in this study agree well in terms of direction and magnitude with the higher fluxes of C at the invaded site as identified by the eddy covariance tower measurements. However, the results here differ from the eddy-covariance based estimates in one important aspect. The biometric results indicate that aboveground carbon accumulation at Ola'a is more than double that at Thurston. The eddy covariance results find that NEE, which is a measure of total change in carbon storage include above- and below-ground pools, is slightly higher at Thurston.

## CONCLUSIONS:

The biometric assessment of carbon fluxes at the two study sites agree in most aspects with those of the tower-based measurements, and therefore, provide support for the tower-based analysis.

## References Cited

- Arcand N, Kagawa A, Sack L, Giambelluca TW (2008) Scaling of frond form in Hawaiian tree fern *Cibotium glaucum*: Compliance with global trends and application for field estimation. *Biotropica* 40: 686–691.
- Asner GP, Hughes RF, Mascaro J, Uowolo AL, Knapp DE, Jacobson J, Kennedy-Boudoin T, Clark JK (2011) High-resolution carbon mapping on the million-hectare Island of Hawaii. *Frontiers in Ecology and the Environment* 9: 434–439.
- Bahn M, Reichstein M, Davidson EA, Grünzweig J, Jung M, Carbone MS, Epron D, Misson L, Nouvellon Y, Rouspard O, Savage K, Trumbore SE, Gimeno C, Curiel Yuste J, Tang J, Vargas R, Janssens IA (2010) Soil respiration at mean annual temperature predicts annual total across vegetation types and biomes. *Biogeosciences* 7 (7):2147–2157.
- Giardina CP, Ryan MG (2002) Total belowground carbon allocation in a fast growing *Eucalyptus* plantation estimated using a carbon balance approach. *Ecosystems* 5:487–499.
- Högberg P, Nordgren A, Buchmann N, Taylor AFS, Ekblad A, Högberg MN, Nyberg G, Ottosson-Lofvenius M, Read DJ (2001) Large-scale forest girdling shows that current photosynthesis drives soil respiration. *Nature* 411 (6839):789–792.
- Janssens IA, Kowalski AS, Ceulemans R (2001) Forest floor CO<sub>2</sub> fluxes estimated by eddy covariance and chamber-based model. *Agric For Meteorol* 106:61–69.
- Litton CM, Giardina CP, Albano JK, Long MS, Asner GP (2011) The magnitude and variability of soil-surface CO<sub>2</sub> efflux increase with temperature in Hawaiian tropical montane wet forests. *Soil Biology & Biochemistry* 43:2315–2323.
- Litton CM, Raich JW, Ryan MG (2007) Review: Carbon allocation in forest ecosystems. *Global Change Biol* 13:2089–2109.
- Litton CM, Ryan MG, Knight DH (2004) Effects of tree density and stand age on carbon allocation patterns in postfire lodgepole pine. *Ecol Appl* 14 (2):460–475.
- Luyssaert S, Reichstein M, Schulze ED, Janssens IA, Law BE, Papale D, Dragoni D, Goulden ML, Granier A, Kutsch WL, Linder S, Matteucci G, Moors E, Munger JW, Pilegaard K, Saunders M, Falge EM (2009) Toward a consistency cross-check of eddy covariance flux-based and biometric estimates of ecosystem carbon balance. *Global Biogeochem Cyc* 23, GB3009, doi:10.1029/2008GB003377.
- Malhi Y, et al. (2004). The above-ground coarse wood productivity of 104 Neotropical forest plots. *Global Change Biol* 10: 563–591.
- Mascaro J, Litton CM, Hughes F, Uowolo A, Schnitze SA (2011) Minimizing bias in biomass allometry: Model selection and log-transformation of data. *Biotropica* 43: 649–653.
- Raich JW, Russell AE, Vitousek PM (1997) Primary productivity and ecosystem development along an elevational gradient on Mauna Loa, Hawaii. *Ecology* 78: 707–721.
- Ryan MG, Law BE (2005) Interpreting, measuring, and modeling soil respiration. *Biogeochemistry* 73:3–27.
- Xu M, DeBiase TA, Qi Y, Goldstein A, Liu ZG (2001) Ecosystem respiration in a young ponderosa pine plantation in the Sierra Nevada Mountains, California. *Tree Physiol* 21 (5):309–318.



### Task 3: Leaf Ecophysiological Characteristics of Native and Non-native Trees at Thurston and Ola‘a Field Sites and Implications for Future Changes in Ecosystem Fluxes

#### PURPOSE AND OBJECTIVES

Forests with different species compositions respond differently to environmental variables largely due to species-specific leaf gas exchange traits (Law et al., 2000).

Because of their different evolutionary histories, structural characteristics, and preliminary evidence of contrasting ecosystem fluxes, it was hypothesized that native species *M. polymorpha* and the invasive non-native species *P. cattleianum* would differ in the leaf-scale ecophysiological traits and that the replacement of canopy leaves by those of *P. cattleianum* would alter the carbon and water exchange between the forest and the atmosphere. To investigate the ecophysiology of these two species, their leaf-scale traits were measured and evaluated together with stand-scale gas exchange under both dry and wet leaf surface conditions. Leaf-level measurements were used both to support the modeling of the responses to climate change as a method of projecting future changes, and to allow us to understand the processes underlying the different ecohydrological responses to climatic change and the differences between native and non-native forests, taking into account the evolutionary background of each species' adaptation to the original habitat.

#### ORGANIZATION AND APPROACH:

The key parameters that strongly determine carbon and water exchange are photosynthetic capacity represented by the maximum rate of RuBP carboxylation ( $V_{\text{cmax}}$ ) and the water use efficiency represented by  $m$  in Ball et al. (1987). These values were obtained for *M. polymorpha* at the Thurston study site and for *M. polymorpha* and *P. cattleianum* at the Ola‘a site. Measurements were made throughout the diurnal cycle at each site using an LI-6400XT (LiCor, Inc., Lincoln, NE, USA) Portable Photosynthesis System. These measurements were used in a multi-layer model (Leuning et al. 1995) to estimate gas exchange rates for three cases (Table 1).

Table 1. Cases for the model computation of stand-scale gas exchange.

Environment	Inputs of leaf traits		LAI		Leaf wetness effects
	TH	OL	TH	OL	
Case 1	<i>M. polymorpha</i>	<i>P. cattleianum</i>	5.75	4.8	Not considered
Case 2	<i>M. polymorpha</i>	<i>P. cattleianum</i>	5.75	4.8	Considered
Case 3	<i>P. cattleianum</i>	<i>M. polymorpha</i>	5.75	4.8	Considered

#### PROJECT RESULTS:

The meteorological and related environmental time series used to scale up leaf level measurements were derived from tower measurements at each site (Figure 1). Measured photosynthetic traits were not consistently different between species (Figures 2 and 3). Under wet leaf surface conditions, both species reduced stomatal conductance to 50-60 % of the level under the similar light intensities and dry leaf surface conditions. Based on the Leuning et al. (1995) multilayered model, simulated stand-scale gas exchange rates for CO<sub>2</sub> and water vapor did not differ between species (Figure 4). Results suggest that changes in leaf ecophysiological traits alone due to the invasion of *P. cattleianum* would not necessarily alter the gas exchange of the

forests in this region, suggesting that differences found at other scales is caused by other factors, such as differences in leaf area or in the relative contributions of overstory and understory canopies.

The multilayer model showed the strong dependence of gas exchange rates on daily PAR, suggesting that future increase in PAR would increase both water vapor and CO<sub>2</sub> fluxes. Transpiration rates depended on the daily mean relative humidity, rather than VPD, and explained the scatter of transpiration rates – PAR relationship. These sites with different dominant species had similar leaf-level ecophysiological traits, and therefore, the response in net photosynthesis and transpiration rates were identical.

#### **ANALYSIS AND FINDINGS:**

Because of the asymptotic increase in net photosynthesis with increase in PAR, increase in net photosynthetic rates due to increased PAR would be modest even in the case of +4.8 % (Future scenario 2, dry season). Increase in mean net photosynthesis with increase in PAR was only 1.4 and 1.6% from the current level for Thurston and Ola'a, respectively.

For transpiration rates, increase with increased PAR by 4.8% resulted in 5.6 and 7.8%, for Thurston and Ola'a, respectively, suggesting the promotion of transpiration rates. Estimated transpiration rate was, however, only 0.77 mm day<sup>-1</sup> and 0.90 mm day<sup>-1</sup> for Thurston and Ola'a (280.0 and 327.5 mm yr<sup>-1</sup>). If the contribution of interception evaporation to evapotranspiration rates of these ecosystems, enhancement of transpiration by increased PAR may be offset by the reduced interception evaporation due to reduced precipitation.

#### **CONCLUSIONS:**

Leaf level characteristics for the principal native and non-native tree species at the study sites are surprisingly similar and, therefore, cannot explain the observed differences in stand level fluxes. Fluxes are sensitive to changes in solar radiation. However, projected changes will produce only modest increase in photosynthesis and transpiration.

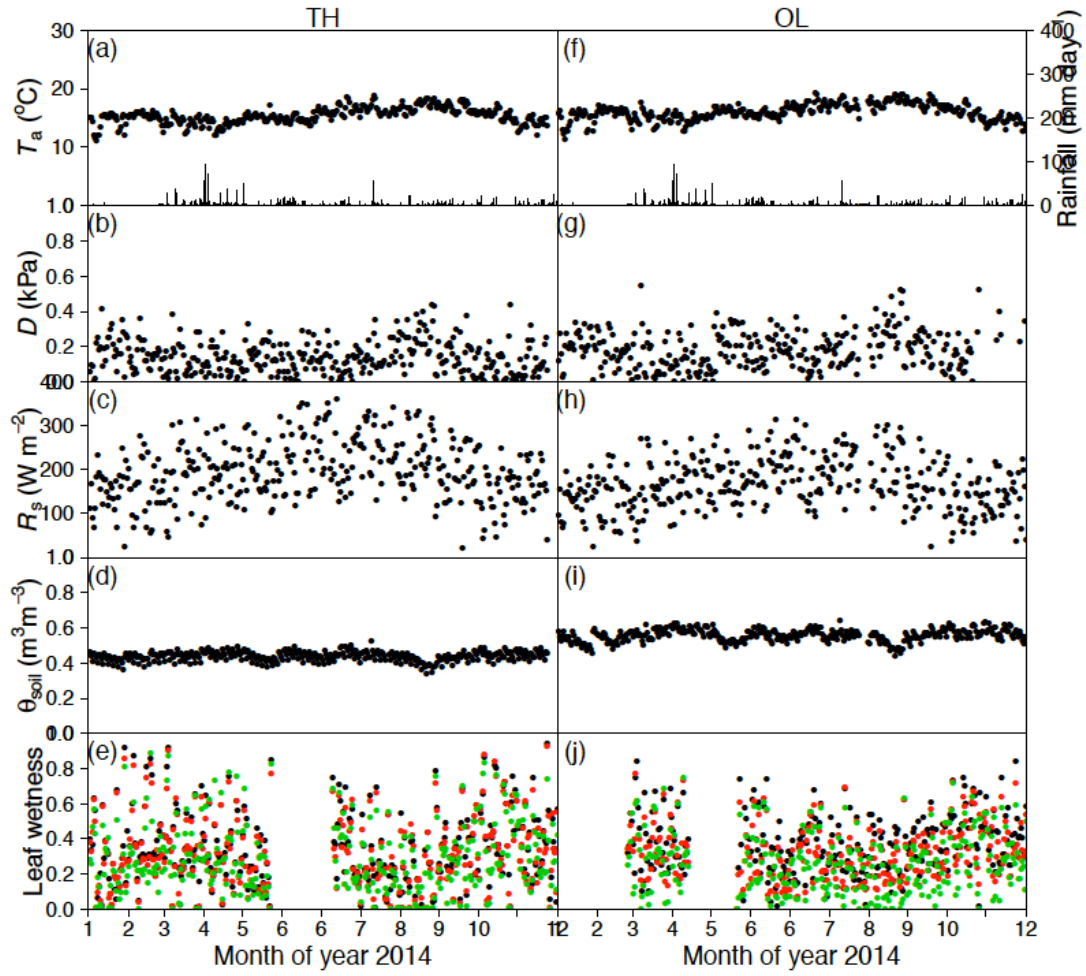


Figure 1. Climate data of Thurston (TH) and Ola'a (OL) sites for (a, f) air temperature ( $T_a$ ) and rainfall, (b, g) air vapor pressure deficit ( $D$ ), (c, h) solar radiation ( $R_s$ ), (d, i) volumetric soil water content of from the surface to 1m depth and (e and j) the outputs from leaf wetness sensor, which increases with leaf wetness between 0 (dry) and 1 (wet) for upper (black), middle (red) and lower (green) canopy.

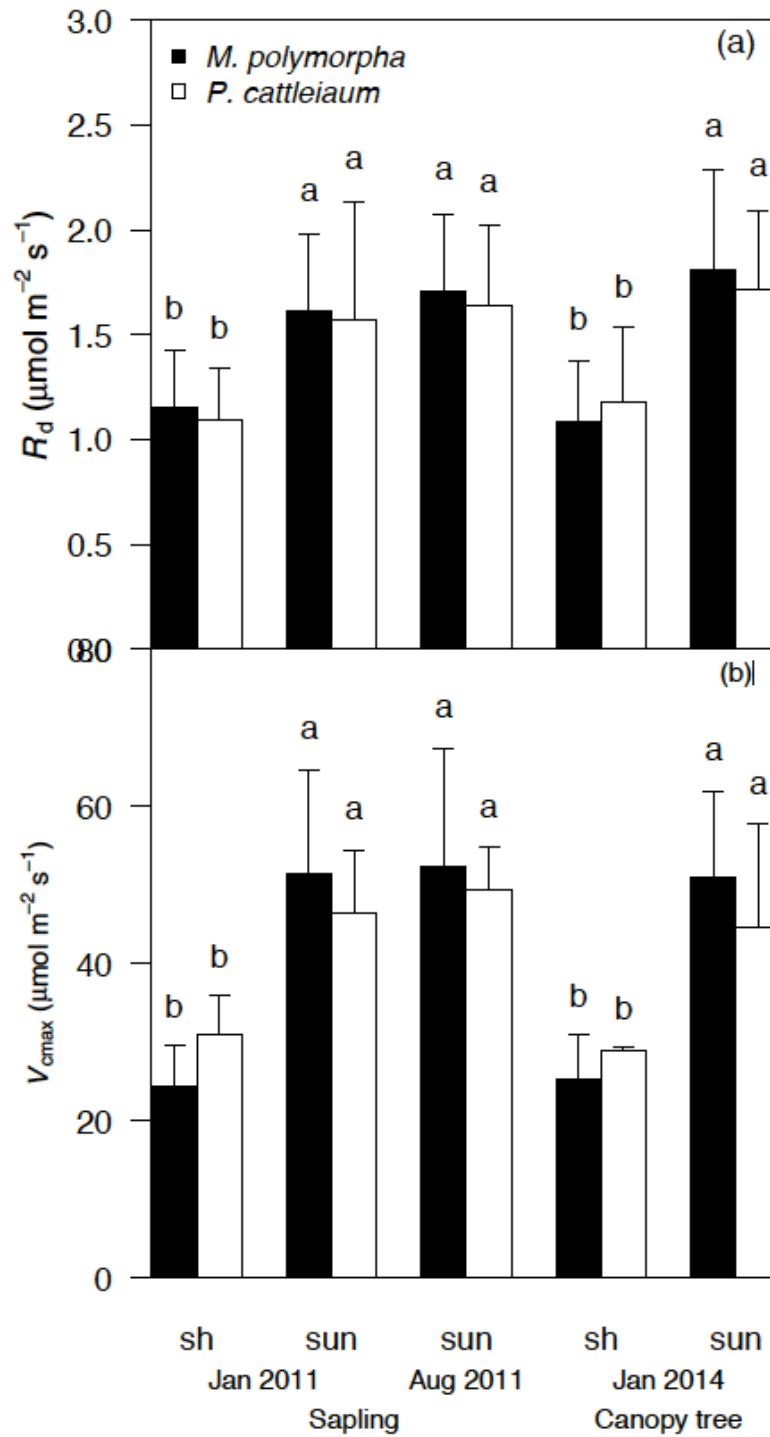


Figure 2. (a) Dark respiration rates ( $R_d$ ) and (b) photosynthetic capacity represented by the maximum rate of RuBP carboxylation by Rubisco ( $V_{\text{max}}$ ) for shaded and sun-exposed leaves of saplings and canopy trees. Vertical bars indicate standard deviation. Values with the same letter are not significantly different at  $p = 0.05$ .

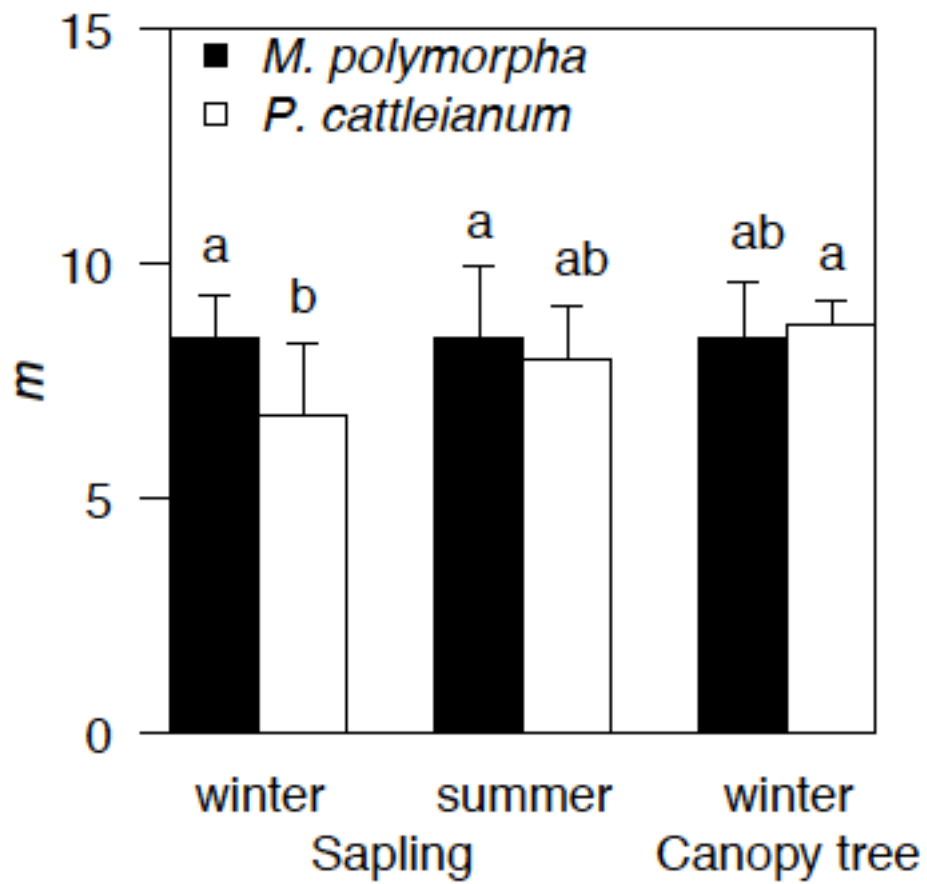


Figure 3. Stomatal sensitivity (Ball-Berry's  $m$ ) of sun-exposed leaves for leaves of saplings and canopy trees. Vertical bars indicate standard deviation. Values with the same letter are not significantly different at  $p = 0.05$ .

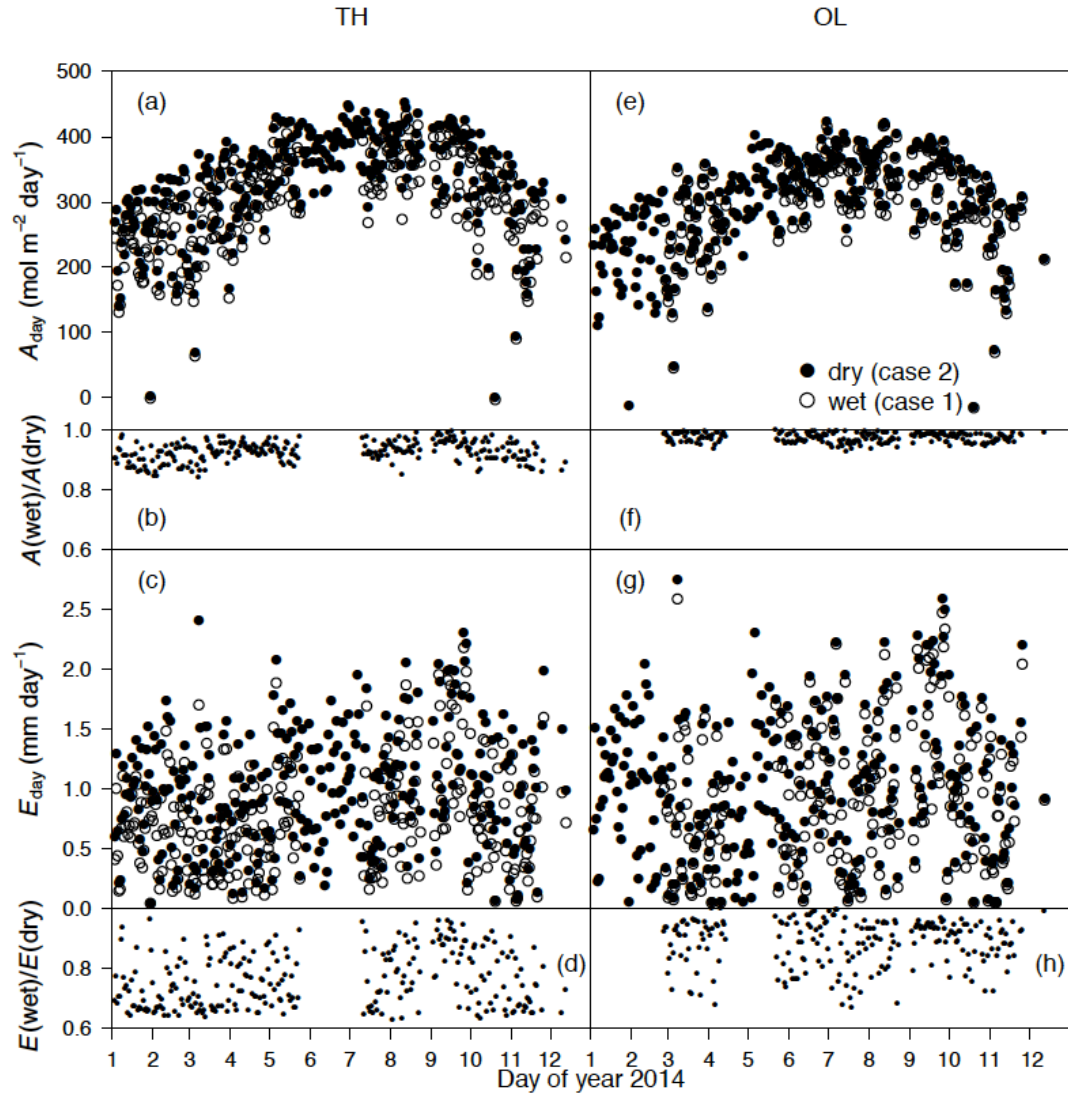


Figure 4. Modeled stand-scale gas exchange rates of (a, e) daily net photosynthesis ( $A_{\text{day}}$ ) and (c, g) daily transpiration ( $E_{\text{day}}$ ). Closed circles in (a,c,e,g) represent the gas exchange rates of cases 1, in which gas exchange rates were computed on the assumption of the absence of leaf wetness effects on  $g_{\text{sw}}$  throughout a year; closed symbols represent the values that were calculated for case 2 where leaf wetness reduces stomatal conductance. (b, f) the ratio of  $A_{\text{day}}$  values and (d, h)  $E_{\text{day}}$  values in case 2 to those in case 1.

## References Cited

- Ball, J.T., Woodrow, I.E., and Berry, J.A. 1987. A model predicting stomatal conductance and its contribution to the control of photosynthesis under different environmental conditions. *Progress in Photosynthesis Research* (ed. I. Biggins), pp. 221-224. Martinus Nijhoff Publishers, Netherlands.
- Law, B.E., Williams, M., Anthoni, P.M., Baldocchi, D.D., and Unsworth, M.H. 2000. Measuring and modelling seasonal variation of carbon dioxide and water vapour exchange of a pinus ponderosa forest subject to soil water deficit. *Global Change Biology* 6: 613-630.
- Leuning, R., Kelliher, F.M., de Pury, D.G.G., and Schulze, E.D. 1995. Leaf nitrogen, photosynthesis, conductance and transpiration - scaling from leaves to canopies. *Plant Cell Environment* 18: 1183-1200.

## Task 4: Implementation of the Community Land Model to Simulate Present and Future Ecosystem Fluxes at the Thurston and Ola‘a Study Sites

### PURPOSE AND OBJECTIVES:

The objective of the proposed study is to determine how projected changes in temperature, precipitation and other climate variables will influence stand growth rates and water use within two of Hawai‘i’s most prevalent plant communities: ‘ōhi‘a (*Metrosideros polymorpha*)-dominated, and strawberry guava (*Psidium cattleianum*)-dominated (the most extensive invaded forest type in Hawai‘i) stands. Quantifying the relative responses of these two dominant forest types (and their underlying keystone species) to shifts in climate will be directly relevant to land conservation planning and restoration efforts and will enable more effective allocation of scarce resources in efforts to conserve forests and protect watersheds.

The Community Land Model (CLM) consists of state-of-the-art sub-modules contributed by the land surface, hydrologic, and ecosystem modeling communities to represent important biogeophysical, biogeochemical, and ecosystem processes, including runoff generation, soil hydrology and thermodynamics, groundwater dynamics, carbon and nitrogen cycling, and ecosystem dynamics. It is therefore well-suited for this study.

### ORGANIZATION AND APPROACH:

To achieve the objective, Version 4.5 of the Community Land Model with prognostic carbon and nitrogen cycles (CLM4.5 hereinafter) has been configured to simulate ecosystem processes driven by 30-min gap-filled meteorological forcing in the observational period at the two flux tower sites located in the two ecosystems of interest. Soil and vegetation parameters are informed by site observations in Tasks 1-3. Given that the cloud water interception (CWI) is a significant component of the water budget, CWI at both sites were estimated and provided to the model as part of the precipitation.

Through sensitivity analyses on the model and discussion with the field team, the specific leaf area at the canopy top ( $SLA_0$ ) has been identified as one of the most sensitive parameters in the model on which the team has good knowledge based on existing literature and field measurements in the two ecosystems of interest. We therefore conducted an ensemble of model simulations at each of the tower sites using a range of  $SLA_0$  values for the observational period. Specifically, at Thurston, the ecosystem is composed of *M. polymorpha* and understory tree ferns, while at , the ecosystem is composed of *P. cattleianum* and tree ferns that could emerge as canopy trees. Based on knowledge on these tree species, a three member ensemble of simulations were conducted at each site shown in Table 1.

Table 1. CLM 4.5 simulations conducted at the two sites

$SLA_0$ ( $m^2 gC^{-1}$ )	Thurston	Ola‘a
Default	0.012	0.012
Sim. 1	0.011	0.018
Sim. 2	0.025	0.025

In Table 1,  $0.012 m^2 gC^{-1}$  is the default  $SLA_0$  value for tropical evergreen trees in CLM and is used here as a reference. The value  $0.011 m^2 gC^{-1}$  is derived from field observations on *M. polymorpha*,  $0.018 m^2 gC^{-1}$  is based on field observations on *P. cattleianum*, and  $0.025 m^2 gC^{-1}$  is based on field observations on the tree ferns. For each of the simulations, a 200-year period is used to spin up the carbon and nitrogen pools.

The model is then configured to test the sensitivity of ecosystem function to climate change at the two tower sites, using the same ensemble of  $SLA_0$  values. Statistical downscaling of temperature and rainfall from Elison Timm and Fortini (2016) and Elison Timm et al. (2015) were used to develop the scenarios based its projection in the period of 2071-2100 under RCP8.5 (see Task 1). Under these scenarios, we expect a temperature change of +3.5°C, and changes in wet (Nov-Apr) and dry (May-Oct) precipitation of 0% to -20% and -30% to -50%, respectively. Changes in solar radiation and relative humidity were estimated by relating present-day monthly variations in photosynthetically active radiation (PAR) and relative humidity (RH) to variations in rainfall at Thurston Tower. The resulting sensitivities are very low for RH. The association between solar radiation and rainfall is greater, e.g., for a 50% decrease in rainfall, PAR would increase by 4.8%. Based on these estimates, two future scenarios are applied to perturb the current-day meteorological forcing at each site as follows:

Variable of interest	Scenario 1				Scenario 2			
	$T_{air}$	P	RH	R	$T_{air}$	P	RH	R
Wet season (Nov-Apr)	+3.5°C	0%	0%	0%	+3.5°C	-20%	0%	+1.9%
Dry season (May-Oct)	+3.5°C	-30%	0%	+2.9%	+3.5°C	-50%	0%	+4.8%

where  $T_{air}$ , P, RH, and R stand for the air temperature, precipitation, relative humidity, and incident short wave radiation, respectively. The scenarios are then applied to perturb the present-day 30-min meteorological forcing and provided to CLM4.5 to quantify changes in water, energy, and carbon budgets.

Figure 1 shows the gap-filled meteorological forcing in the observational period and the two future scenarios by applying the proposed percent changes to the observed forcing at Thurston and Ola'a. Although the sites are close to each other geographically, differences in meteorological variables are significant due to spatial heterogeneity in clouds and precipitation as a result of orographic rising of moist air mass.

## PROJECT RESULTS:

Figures 2 and 3 show the simulated monthly energy and carbon fluxes at Thurston and Ola'a, with comparison to observations. At each site, the ensemble of simulations, with perturbations on  $SLA_0$ , generally provide an envelope to bracket observed energy and carbon fluxes. Specifically, at Thurston, net radiation is well captured by the model in all simulations. Latent heat is better captured by the simulation with  $SLA_0 = 0.25$ , suggesting that tree ferns might be dominating the evapotranspiration. All simulations underestimate sensible heat fluxes significantly, while ground heat fluxes are slightly underestimated. The net ecosystem exchange and gross primary production seem to vary within the range of the three simulations. At Ola'a, net radiation seems to be underestimated, suggesting that the albedo of the ecosystem (i.e., composed of *P. cattleianum* and tree ferns) at Ola'a might needs to be better characterized. Latent heat is generally well captured by all simulations but the default simulation seems to be able to better capture the peak. Similar to those in Thurston, sensible and ground heat fluxes are overestimated. NEE and GPP at Ola'a are better captured by the simulation with the default parameter.

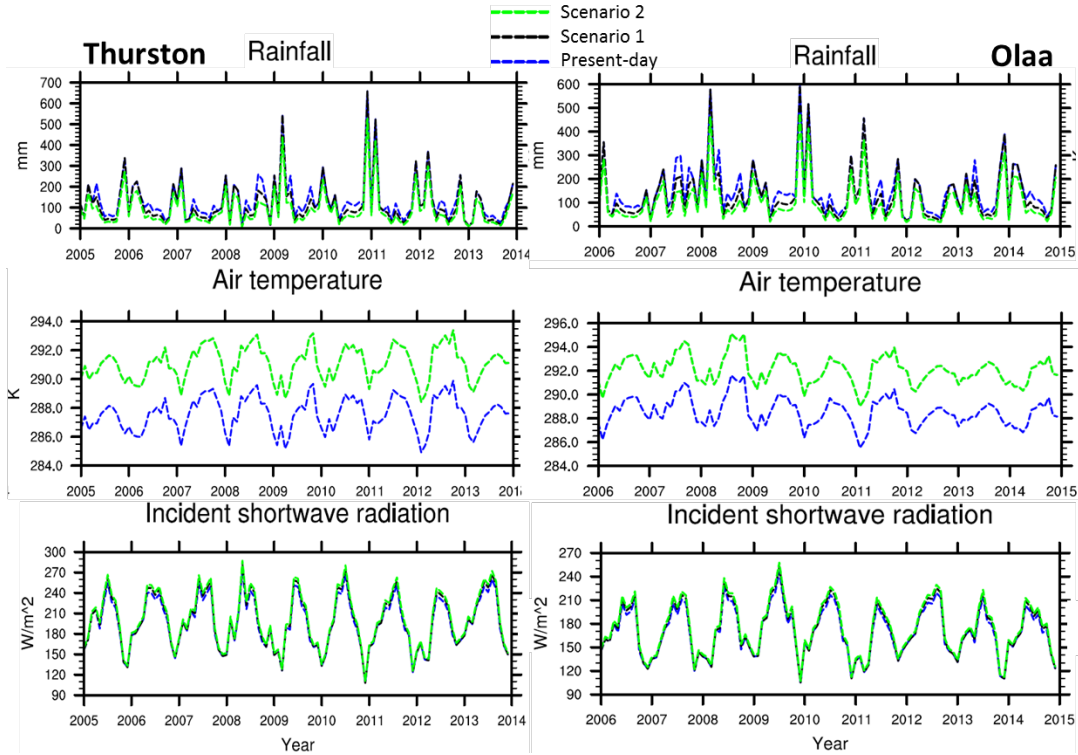


Figure 1. Observed meteorological forcing and the two future climate scenarios used to drive CLM simulations at Thurston (left panels) and Ola'a (right panels).

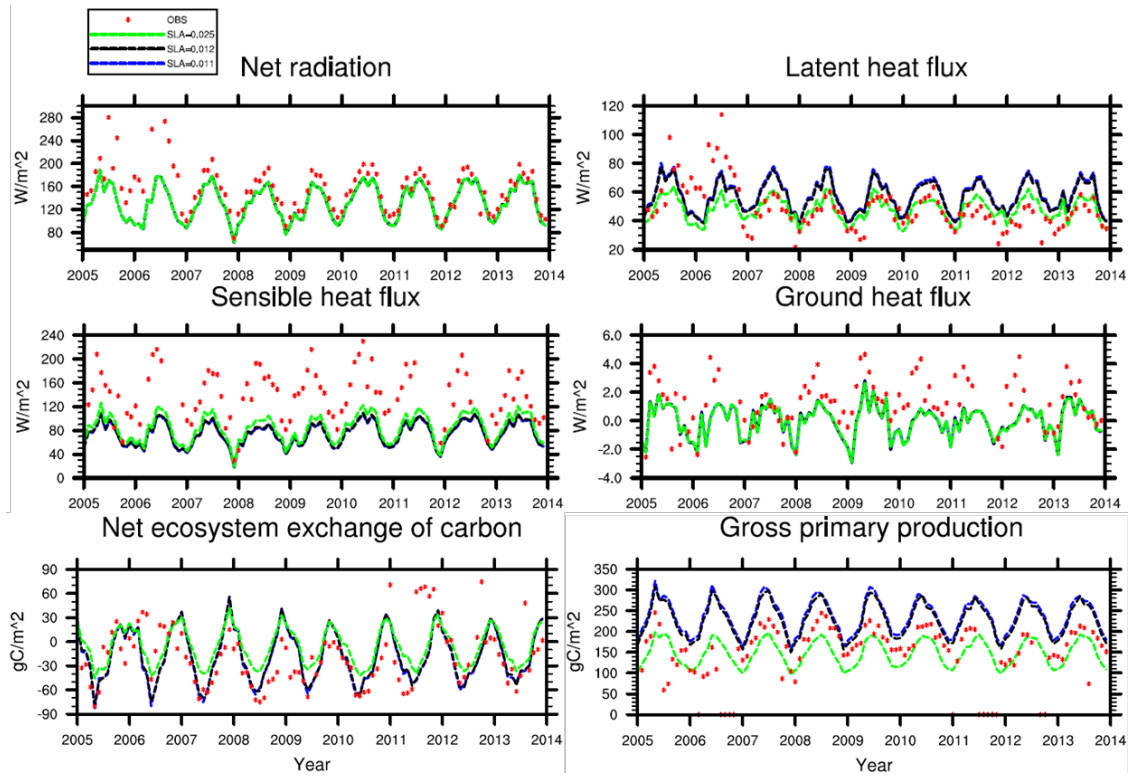


Figure 2. Simulated energy and carbon fluxes at Thurston with comparison to tower observations

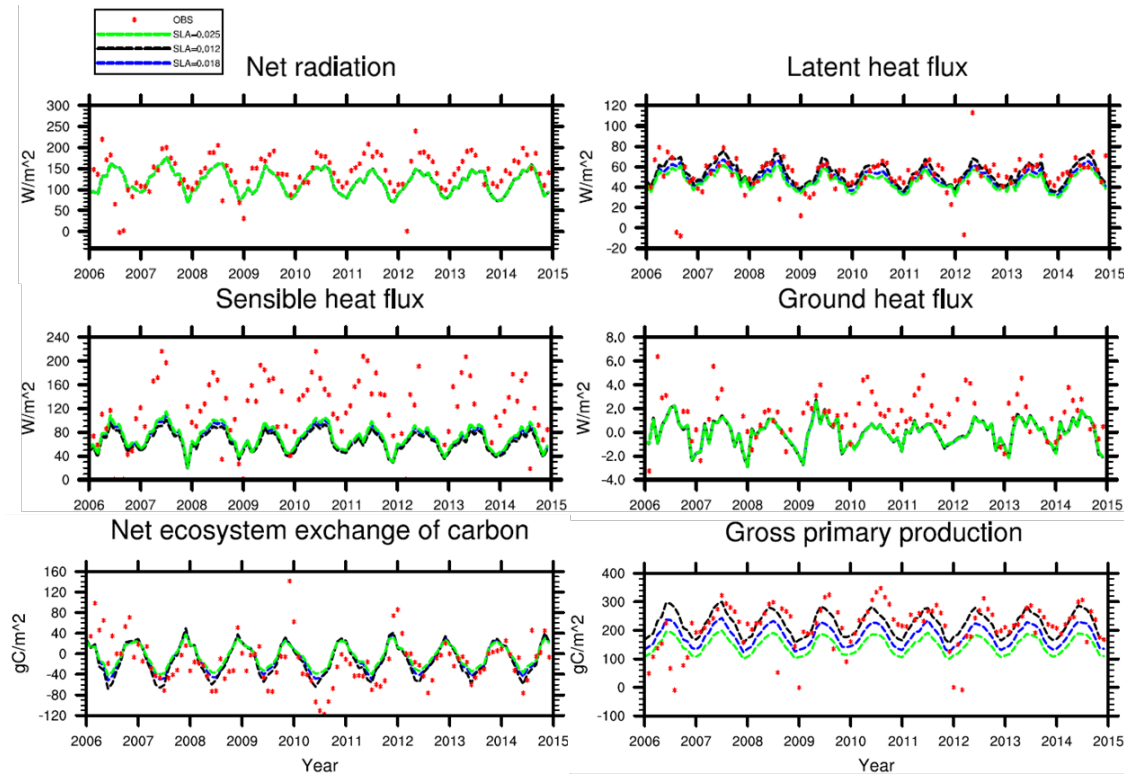


Figure 3. Simulated energy and carbon fluxes at Ola'a with comparison to tower observations. As all simulations with different SLA<sub>0</sub> perturbations seem to capture the observations in some aspects, we forced all ensemble members under the two proposed future scenarios to quantify the uncertainty range of simulated NEE, GPP, LH. In addition, we added the simulated total runoff (Q) for a complete assessment of potential impacts of climate change. It is obvious that projected climate change will likely turn both ecosystems to small carbon sinks. GPP at both sites will increase however, indicating elevated total ecosystem respiration in response to climate change. In terms of the hydrologic fluxes, latent heat are expected to slightly increase at both sites, in response to increase in incident shortwave radiation, while total runoff are predicted to significantly decline at both sites, suggesting a potential significant shift in hydrologic regime in watersheds on the Big Island.

Table 2. Mean annual simulated fluxes at Thurston in the observational period and under future scenarios.

Scenario	NEE (gC m <sup>2</sup> yr <sup>-1</sup> )			GPP (gC m <sup>2</sup> yr <sup>-1</sup> )			LE (W m <sup>2</sup> )		
SLA <sub>0</sub>	default	Sen1	Sen2	default	Sen1	Sen2	default	Sen1	Sen2
Present	-194.55	-212.74	-71.68	2739.9	2848.3	1776.9	56.77	58.01	48.11
Scenario 1	-145.99	-169.26	-39.00	2939.1	3065.7	1926.3	60.64	61.98	51.05
Scenario 2	-191.20	-209.10	-69.03	2905.6	3003.7	1936.6	59.58	60.90	49.86

Table 3. Mean annual simulated fluxes at Ola‘a in the observational period and under future scenarios.

Scenario	NEE (gC m <sup>2</sup> yr <sup>-1</sup> )			GPP (gC m <sup>2</sup> yr <sup>-1</sup> )			LE (W m <sup>2</sup> )		
SLA <sub>0</sub>	default	Sen1	Sen2	default	Sen1	Sen2	default	Sen1	Sen2
Present	-148.22	-91.78	-59.28	2685.7	2168.2	1771.1	54.10	49.50	46.52
Scenario 1	-68.53	-28.17	-18.24	2819.1	2284.0	1890.2	55.64	50.73	47.62
Scenario 1	-114.45	-59.61	-41.17	2835.5	2298.0	1900.8	55.36	50.21	46.85

Table 4. Summary of observed mean annual fluxes at the sites

Sites	NEE (gC m <sup>2</sup> yr <sup>-1</sup> )	GPP (gC m <sup>2</sup> yr <sup>-1</sup> )	LH (W m <sup>2</sup> )
Thurston	421.45	2222.46	57.80
Ola‘a	341.86	2992.21	61.49

## ANALYSIS AND FINDINGS:

To summarize, based on modeling results described in the previous section, we have the following findings that point to potential directions to improve the results:

1. Tree ferns seem to be a significant ecosystem component at Thurston. Observed fluxes seem to be enveloped by simulations with SLA<sub>0</sub> values vary between *M. polymorpha* and the tree ferns. Our next step will be to assess the fractional areas of these species within the tower footprint to improve the results.
2. The default parameter values seem to work well at Ola‘a, but the albedo in that specific ecosystem needs to be better quantified.
3. Projected climate change will likely have significant impacts on carbon and water cycles in both ecosystems.

## CONCLUSIONS AND RECOMMENDATIONS:

The findings are encouraging and we will perform more sensitivity analyses in the near future, targeting a paper focusing on “Responses of water, energy, and carbon dynamics of Hawaiian native and non-native ecosystems to climate change”, with recommendations on resources management.